DP-1341

662906

PROGRESS REPORT DOSE-TO-MAN PROGRAM FY 1973

T. V. CRAWFORD

JANUARY 1974

E. I. du Pont de Nemours & Co.
Savannah River Laboratory
Aiken, S. C. 29801

PREPARED FOR THE U. S. ATOMIC ENERGY COMMISSION UNDER CONTRACT AT(07-2)-1

Printed in the United States of America
Available from
National Technical Information Service
U. S. Department of Commerce
5285 Port Royal Road
Springfield, Virginia 22151
Price: Printed Copy $5.45; Microfiche $1.45

662906

DP-1341
UC-11

PROGRESS REPORT
DOSE-TO-MAN PROGRAM

by

T. V. Crawford, Compiler

Contributing Authors

R. E. Cooper
T. V. Crawford
M. M. Pendergast
E. L. Wilhite

Approved by
T. V. Crawford, Research Manager
Environmental Transport Division
Savannah River Laboratory

January 1974

E. I. du Pont de Nemours & Co.
Savannah River Laboratory
Aiken, S. C. 29801

PREPARED FOR THE U. S. ATOMIC ENERGY COMMISSION UNDER CONTRACT AT(07-2)-1

ABSTRACT

The Dose-to-Man Program at the Savannah River Plant (SRP) was conceived in FY-1972 and operations began in FY-1973. The major objectives of the program are to develop (or adapt), test, and apply comprehensive mathematical models to calculate the dose-to-man from one or more point sources via atmospheric and aqueous releases. These models will be applied to SRP operations; however, the methods are expected to be generally applicable over a large portion of the southeastern United States.

This report presents a discussion of a new meteorological data acquisition program now in operation using a 1200-ft TV-tower located near the plant site and seven 200-ft towers to be located onsite in FY-1974. Previously collected meteorological data from the TV-tower have been analyzed to show spatial and temporal variation in eddy diffusivity, mesoscale kinetic energy spectra, and dispersion climatology based upon wind-sequencing information. This report also presents a discussion of a framework for calculation of dose-to-man, and a comparison of the Brookhaven National Laboratory (BNL) and Pasquill methods for determining dispersion coefficients. A current sulfur dioxide survey is discussed which will help verify the calculation techniques for predicting dispersion from heated plumes.

FOREWORD

The Dose-to-Man program is a new effort at the Savannah River site to conduct multi-discipline applied research on the mechanisms by which material discharged into the environment eventually reaches man. This first year was one of staffing, developing facilities, and starting research in the atmospheric sciences. This report presents some history of the Dose-to-Man program, a description of the Savannah River site, atmospheric science research facilities, and a series of short articles on research completed or under way.

Todd V. Crawford, Research Manager
Environmental Transport Division

CONTENTS

LIST OF FIGURES

LIST OF FIGURES (CONTINUED)

LIST OF FIGURES (CONTINUED)

LIST OF FIGURES (CONTINUED)

LIST OF TABLES

INTRODUCTION

The Dose-to-Man Program was conceived in FY-1972 and began functioning in FY-1973. The major objectives of the new program are to develop (or adapt), test, and apply comprehensive mathematical models to calculate the dose-to-man from the releases from one or more point sources via atmospheric and aqueous vectors, and to apply these methods to Savannah River Plant (SRP) operations.

The program is located at SRP, one of the AEC's major production sites. SRP encompasses a fuel manufacturing facility, three large production reactors, two large chemical reprocessing plants, a heavy water production plant, and various waste management activities. These facilities are located on a 300 square-mile site south of Aiken, South Carolina.

Comprehensive site surveys were made prior to startup of the facilities, and extensive environmental monitoring has been continued since the start of operation. However, the need still exists to develop models leading to an understanding of environmental processes that take place between the location of the unavoidable small releases of radioactivity and the receptors some distance away. This understanding will lead to the further development of more sophisticated mathematical models to provide a basic methodology for predicting the effects of activity releases at SRP.

The development of improved models for calculating the effects of activity releases at large distances is particularly important now because concerns have shifted to small dose levels and to population doses, and because commercial nuclear activities are rapidly developing in the southeastern United States. Within a 200-mile radius of SRP there are now more than 10 large power reactors completed or committed, two fuel fabrication plants, a commercial chemical reprocessing plant under construction, and a private waste storage site under consideration. Thus, within the southeastern United States, the environment will soon be receiving input from a variety of nuclear activities.

The Dose-to-Man Program will require a multi-disciplined effort capable of understanding, modeling, and then verifying the modeling, of all of the significant transport pathways from production to uptake by people. However, the initial focus is in the atmospheric sciences as previous work has identified the atmosphere

as the main pathway for material to contribute to population doses. Previous potential dose calculations, safety studies, postulated accident situations, etc. have used plume dispersion methods developed by Brookhaven National Laboratory (BNL) together with a two-year data base collected from a nearby 1200-ft television tower. As concern shifts to the shared environment of the Southeast, atmospheric transport, diffusion, and deposition techniques must be developed and applied to this space scale. Non-radioactive materials are being investigated as well as radioactive materials.

Besides techniques applicable to routine releases of materials, the program also involves improving the capability to evaluate the potential consequences of an accidental release.

The program provides interaction with SRP personnel to facilitate incorporation of the Dose-to-Man research findings into SPR plans. Onsite, the program involves cooperative effort between the Savannah River Laboratory (SRL) and SRP, the Savannah River Ecology Laboratory (SREL), and the Savannah River Operations Office of the Atomic Energy Commission (SROO-AEC) (including the programs developed under the auspices of the National Environmental Research Park); offsite, the research results should be broadly applicable also.

Cooperative efforts with other Atomic Energy Commission (AEC) laboratories are being planned to cover areas of mutual interest. The close association of this program with production activities at SRP hopefully will identify problem areas which other AEC laboratories could help solve.

A large part of this first year's effort has gone into planning programs, staffing, developing meteorological research facilities, developing computer codes to handle and analyze data, and initiating a variety of research projects.

In addition to starting the research effort, the Dose-To-Man staff has spent a significant amount of time on site environmental reports, on safety studies relevant to plutonium handling and hydrogen sulfide emissions, and on improving methods for predicting the extent and effects of accidental releases at SRP. Joint tests are being planned with the Lawrence Livermore Laboratory (LLL) to evaluate improved methods of calculating the consequences of accidental releases to the atmosphere.

This first report for the Dose-to-Man Program at SRP discusses the organization, meteorological research facilities, and research in progress.

The Dose-To-Man Program is funded by the Division of Biomedical and Environmental Research (DBER) and the Division of Production and Materials Management (DPMM) of the AEC.

ORGANIZATION

The Savannah River Plant site is administered by the Savannah River Operations Office (SROO) of the AEC which is physically located onsite. The site facilities are operated by the Atomic Energy Division (AED) of the E. I. du Pont de Nemours and Co. under contract with the AEC. The Du Pont company designed and built the facilities in the early 1950's and has operated the facilities since construction.

The Savannah River Plant (SRP) organization operates the various production facilities and employs about 5000 people. The Savannah River Laboratory (SRL), with about 900 people, is an applied research laboratory which exists primarily to support SRP. The major fraction of the SRL effort is devoted to developing new or improve existing SRP processes. An advanced computer center and a technical library are also operated by SRL. Environmental research activities are conducted by the Environmental Sciences Section of SRL. The Environmental Sciences Section (ESS) is comprised of two divisions: the Environmental Effects Division (EED) and the Environmental Transport Division (ETD), plus the Environmental Analysis and Planning Group (EAP), which studies the interrelationship between the environment and SRP processes. The EAP evaluates, assesses, and makes recommendations for needed research, procedure changes, process changes, and assists in safety analysis reports, etc. The genesis group (EAP) early recognized the need for the applied research effort now called the Dose-to-Man Program. The Dose-to-Man effort is part of the program of the Environmental Transport Division.

In Addition to the above AEC and Du Pont groups, the University of Georgia operates the SREL on the Savannah River site. In addition to full-time staff members in residence onsite, a number of students participate in a variety of ecological field studies during the summer.

The Savannah River site has also been designated a National Environmental Research Park (NERP) by the AEC, which means that outside groups can request permission to perform research onsite at locations not directly used in production processes by SRP, as long as their proposed activities will not interfere with the main production mission of the site. This program is being administered by SROO-AEC.

1. FACILITIES FOR ATMOSPHERIC SCIENCES RESEARCH

INSTRUMENTED TV TOWER

In 1965-66, a 1200-ft TV tower (Augusta, Georgia, Station WJBF-TV or Channel 6, located at Beech Island, South Carolina, approximately 30 km northwest of the geometrical center of SRP) was instrumented with *Climet** bivane wind systems and platinum resistance thermometers. The objective was to obtain two years of data to perform a variety of safety analyses. This data base was collected between 1966 and 1968 on a punched paper tape recording system with a data sampling frequency of once per 3 minutes.

The tower instrumentation configuration is given in Figure 1-1. Between 1966 and 1972, the tower instrumentation was used only periodically. Beginning in 1972 and continuing into 1973, the system was improved. A four-wire system instead of the old three-wire system is now in use for the temperature measurements to minimize problems from lead resistances. The *Climet* instrumentation has been partially rebuilt to put more of the electronics on the ground for ease of maintenance. New tails have been acquired, the bivane tail performance has been checked in a wind tunnel, and a new data recording system was purchased which utilizes a digital millivolt meter, clock, scanning unit, memory buffer, and magnetic tape. Thirty-two channels of data can easily be recorded at frequencies exceeding the time response of the meterological instrumentation.

A 10-meter tower for collecting near-surface data is located in the vicinity of the TV tower but far enough away from the transmitter building so that the air reaching this tower is representative of the surrounding area. Data at the lower heights are necessary for comparison with data taken during meteorological diffusion studies at other sites. The 10-meter tower was installed during June 1973.

The location of the TV tower, the nearby 10-meter tower, the 1-story transmitter building, and the orientation of the meteorological instrumentation are shown on Figure 1-2.

---

* Tradename of Climet Instruments, Sunnyvale, California

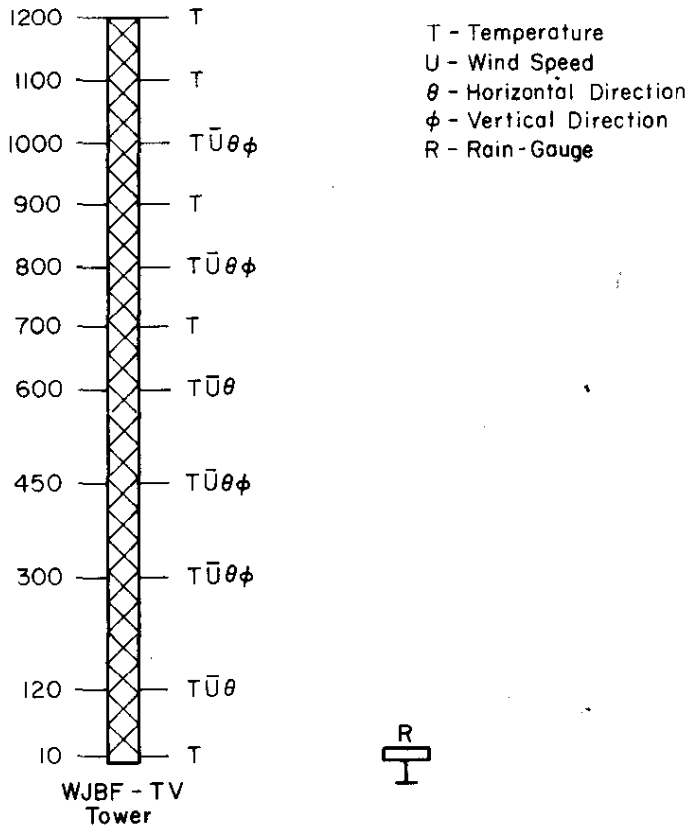

Figure 1-1. Temperature and Wind Instrumentation Elevations (in feet above ground) on WJBF-TV Tower for 1966-72.

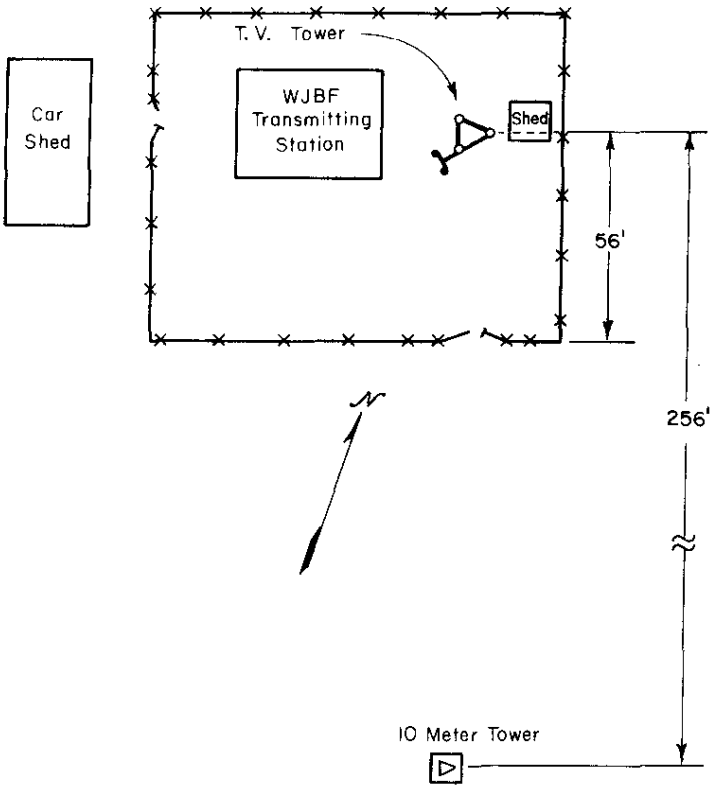

Figure 1-2. Location of Meteorological Instrumentation at the WJBF-TV Transmitter Site.

The new recording system for the TV tower became operational in May 1973 and was used extensively in cooperative studies with North Carolina State University and Pacific Northwest Laboratories during May. Tower instruments for routine data collection were relocated as shown on Figure 1-3. This configuration involves 28 channels of meteorological information in addition to date, time, and reference voltages. All of the instruments are currently sampled and recorded on magnetic tape once per 5 seconds.

Routine operation of the tower provides an ever-increasing data base with better time resolution than was formerly obtainable. Standard deviations of wind direction can now be calculated and applied to current emission data. The Dose-to-Man Program will apply these data to test (and aid in the development of) improved models for dose calculations on a routine release basis and to improve the emergency response capability.

SEVEN-TOWER METEOROLOGICAL SYSTEM

The various production areas on SRP have had wind direction and velocity instrumentation for use in emergencies. These instruments have been operating for many years, and in all cases they are located on relatively short towers on top of the tallest building in the particular operating area. To obtain better quality and more representative wind data, new instrumentation will be installed near each operating area.

The operating areas and the new meteorological tower locations are shown on a map of the SRP site (Figure 1-4). The *Vectorvane** instruments to measure wind direction and velocity are to be mounted 200 ft above the ground to match the height of the major SRP stacks through which effluents are released. The *Vectorvane* instrument has a low starting speed, measures vertical and azimuthal wind directions, and measures speed and direction for the same air parcel. The tower in D-Area will also have a wind instrument at mid-tower height.

The tower locations are representative of the general landscape of the area and are located in typical pine forests about one-half mile from the main buildings in the operating area. The towers are positioned where the prevailing winds do not pass over any buildings before reaching the tower. The data from the towers will be recorded in the adjacent area control rooms and telemetered over telephone lines to a central Weather Center - Analysis Laboratory (WC-AL). The seven-tower system will be complete late in the winter of 1973-74.

* Trademark of Meteorology Research, Inc., Altadena, California.

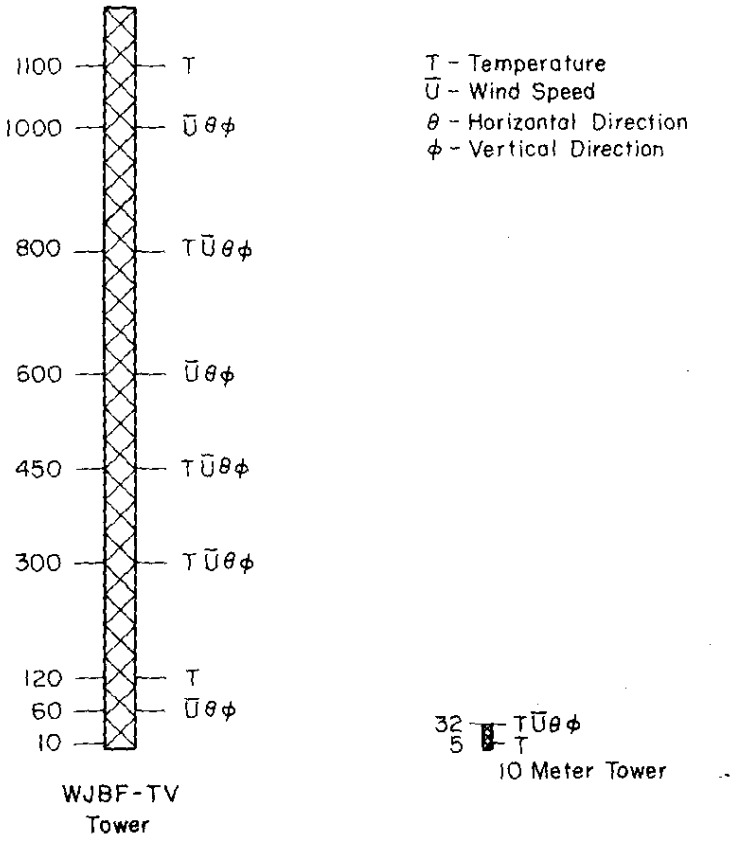

Figure 1-3. Repositioned Meteorological Instrumentation at the WJBF-TV Transmitter Site as of July 1973 (compare with Figure 1-1).

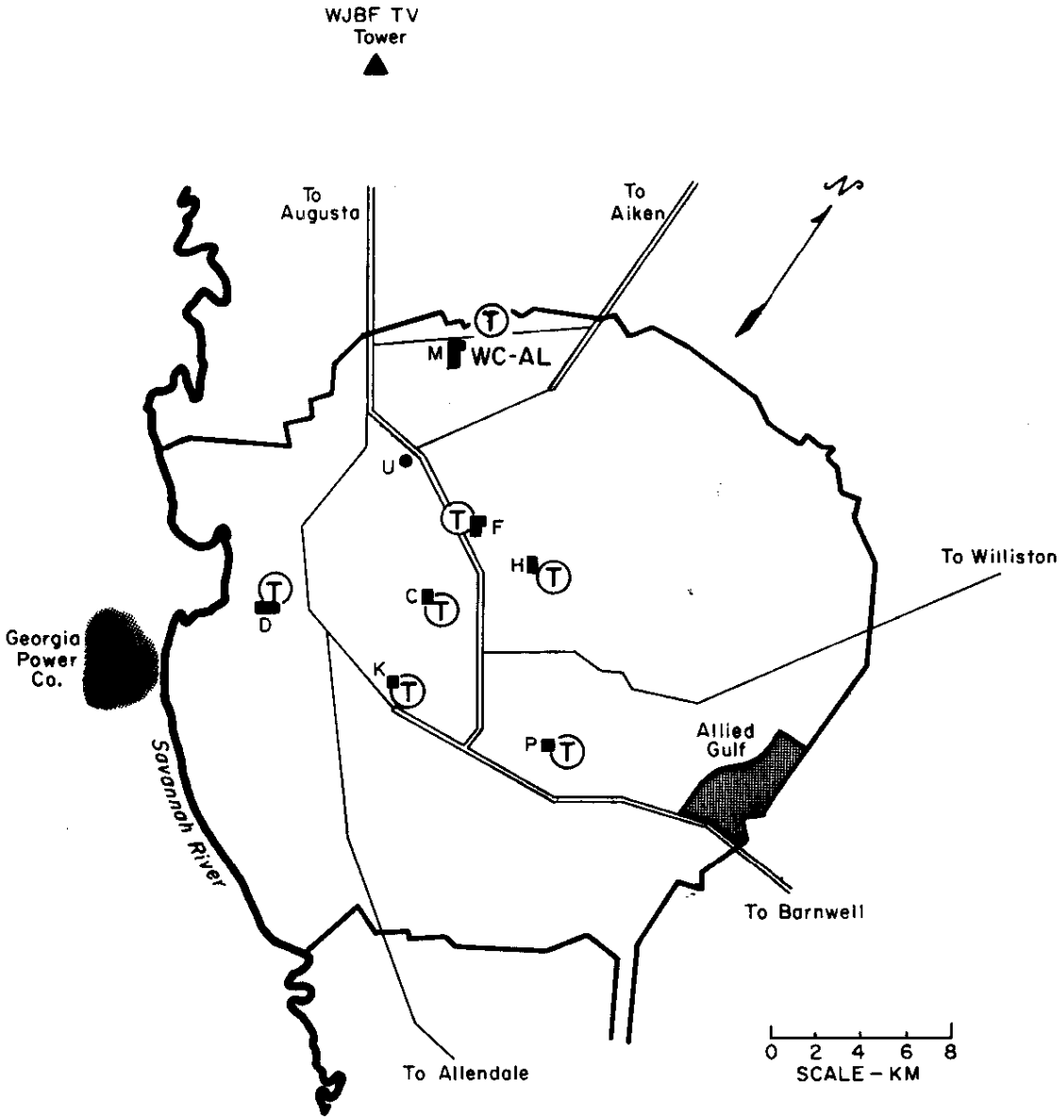

Figure 1-4. Locations of the Seven Area Meteorological Towers, the WJBF-TV Tower, the Weather Center-Analysis Laboratory (WC-AL), and the Wind Tunnel(U).

Adjacent to SRP are the locations of the Allied Gulf Nuclear Fuel Services plant at Barnwell, S. C., and the Georgia Power Company Vogtle reactor site on the opposite shore of the Savannah River. Both of these sites have meteorological towers (Figure 1-4).

THE WEATHER CENTER - ANALYSIS LABORATORY

The Weather Center - Analysis Laboratory (WC-AL), adjacent to the main SRL building, will provide a collection point for site meteorological data, a link with the National Weather Service, a place to develop additional meteorological support for site emergency plans, a data library to support field programs, and a data analysis center. The building was occupied in June 1973, and communications links to the National Weather Service (NAMFACS, Teletype Circuit A and Circuit C) were established. The magnetic tape data recording system from the TV tower will be moved to the WC-AL in the fall of 1973. Data from the TV tower will be received via a telephone link. The data recording system will be expanded to record the data from the seven-tower system on the same tape. By the spring of 1974, all of the site meteorological data will be recorded in real time on the same tape. These basic data will be used in the research program to improve existing methods and to develop new methods for wind analyses.

ACOUSTIC SOUNDER

An acoustic sounder developed and built by the University of Melbourne at Melbourne, Australia, arrived in June 1973. This unit is similar to the one used extensively over the past year at Argonne National Laboratory (ANL) and is identical to two other units recently installed at ANL.

The acoustic sounder sent here was operated for several weeks at ANL. The unit has a height range of 6000 ft, variable frequency from 1 kHz to 2 kHz, a band width of 5 Hz, a transducer input power of 100 watts, and a variable intensity display to measure time and height. The initial use of this instrument will be to compare data from this instrument with temperature and wind speed discontinuities observed on the TV tower. As interpretation and data handling capabilities develop, the acoustic sounder will routinely monitor the depth of the atmospheric mixing layer and will contribute to other research programs.

WIND TUNNEL - METEOROLOGICAL LABORATORY FACILITY

In February 1973, a wind tunnel surplused by the Environmental Protection Agency Laboratory in Las Vegas, Nevada, was acquired for use at the Savannah River site. The tunnel can be operated in either a once-through mode or in a closed-path mode. It has two test sections: one is 2 by 2 by 3-ft-long and the other is 4 x 4 x 6-ft-long. Maximum wind speed capability of the tunnel is 200 mph. The wind tunnel will be used primarily for calibration of instrumentation, but has the capability for model studies of wind patterns and diffusion around buildings.

The wind tunnel is to be placed in operation in Building 704-U early in FY-1974. Building 704-U on the Savannah River site is centrally located (see U-Area, Figure 1-4) and is also the location for the initial checkout of the acoustic sounder.

This same building will contain meteorological instrument storage, calibration, and minor instrument modification facilities.

2. METEOROLOGICAL DATA PROCESSING: COMPARISON OF THE SRL-MODIFIED BNL METHOD WITH PASQUILL CATEGORIES AS DETERMINED FROM TEMPERATURE DATA†

INTRODUCTION

Savannah River Plant (SRP) safety and environmental analyses to date were obtained by processing meteorological data with a modification of methods developed at the Brookhaven National Laboratory (BNL).[1] The Atomic Energy Commission (AEC) has recently issued Safety Guide 23,[2] which specifically advocates the use of a meteorological data reduction scheme based on methods developed by Pasquill.[3] In this report, the two methods are discussed, and comparison calculations are performed to evaluate differences between the two methods.

The Savannah River Laboratory (SRL) meteorological data acquisition program[4] was initiated in 1965. The objective was to obtain sufficient data to characterize atmospheric turbulence as a function of time. Variables measured were temperature, wind speed, horizontal and vertical wind direction, and standard deviation of wind direction. The state of the art for data acquisition systems at that time precluded acquisition rates that would allow numerical calculations of standard deviations (sigmas). Consequently, calculation of sigmas was attempted by analog methods. Even though the analog technique was vastly improved in the course of data acquisition, the measured sigma data were not sufficiently accurate to characterize atmospheric turbulence. Thus, other measured variables were related to the sigmas to obtain the dispersion parameters.

THE BNL METHOD

The method in use at SRL separates the data into stable and unstable conditions. If the temperature gradient were positive with increased height, conditions were classed as stable; otherwise they were classed as unstable. Diffusion parameters were estimated by a power law as

$$\sigma_y = \alpha \sigma_a x^{\beta} \qquad (1a)$$

$$\sigma_z = \alpha \sigma_e x^{\beta} \qquad (1b)$$

---

†Work done by R. E. Cooper.

where σ_a and σ_e are the standard deviations in degrees of the azimuth and elevation angle of wind direction, respectively. Where direct measurements are absent, these parameters are estimated from other data. The constants α and β depend on stability classification, and x is distance downwind in meters. For unstable conditions, σ_a was taken to be a function of measured wind speed, $\tilde{u}$ (meters/second), in accord with observed correlations at BNL for a reference elevation of 100 meters.[1]

$$\sigma_a = (23/\tilde{u}) + 4.75 \qquad (2)$$

A power law wind profile, $u = u_o\left(\frac{z}{z_o}\right)^n$, adjusts the wind speed to other heights (n = 0.25 for unstable, and 0.5 for stable conditions), and the product ($\tilde{u}\ \sigma_a$) is assumed to be constant with height. A constant relationship between σ_a and σ_e was also assumed.

$$\sigma_e = 0.7\ \sigma_a \qquad (3)$$

No correlations were given by BNL for stable conditions; so for SRL analyses, a scheme was devised to provide a continuum of meteorological possibilities to include stable conditions. Noting that a practical lower limit of Equation 2 is about 5° (for unstable condition) and a practical lower limit for σ_a under stable conditions is about 2°, values of σ_a were assigned that were random and evenly distributed bwtween 2° and 5°. In addition, the ratio σ_e/σ_a was randomly assigned but constrained between 0.7 as in Equation 3 and 0.2 as given in Reference 1. Thus, a value of σ_a and σ_e was computed and assigned to each set of meteorological measurements collected during the 2-year period (1966-1968).

THE PASQUILL METHOD

The method used in this comparison is the Gifford[5] graphical presentation of Pasquill's method. Six stability cateogories are considered and expressed in the form of a power law similar to Equation 1.

$$\sigma_y = \alpha_y\ x^{\beta_y} \qquad (4a)$$

$$\sigma_z = \alpha_z\ x^{\beta_z} \qquad (4b)$$

The constants α and β are obtained as fitting parameters for each stability category as tabulated by Tadmor and Gur.[6] Stability classifications were made on the basis of temperature measurements according to Table 2 in Reference 2.

Stability classifications are summarized in Table 2-I. Dispersion parameter derivations are shown schematically in Figure 2-1. There are two basic differences in the methods. The most obvious is the number of stability classifications involved, but the most significant is that the Pasquill method, as described, allows only a single value of σ_y and σ_z at a given distance for a given stability category. The AEC Safety Guide 23 classification is also considered to be ambiguous because no guides are given on the temperature sensor elevations for a particular release, although the temperature gradient is a function of height.

COMPARISON CALCULATIONS

The 1966-68 meteorological data base previously described was processed to obtain joint-frequency χ/Q distributions as a function of distance. Figure 2-2 shows estimates for the 95th percentile value generally used to compare hazards criteria. The BNL method yields results that are about a factor or 2 lower than Pasquill estimates for a release height of 65 meters. Also shown is a comparison of results using data averaged over various time intervals up to 1 hour. At the 95th percentile, the indication is that χ/Q values are lower for longer time averaging.

Annual average estimates presented in Figure 2-3 show about the same relationship as Figure 2-2. Figures 2-2 and 2-3 also indicate variability with respect to distance. All calculations assume infinite mixing depth (no inversion lid).

Both methods are considered to be qualitative approaches in the absence of more-definitive meteorological data. This qualitative approach, together with the undefined mixing depth, requires normalization corrections based on experimental data. Long-term tritium measurements out to a distance of 40 km indicated that the imposition of a constant 300 meter inversion lid produced annual average concentrations in very good agreement with measurements. (This does not imply the existence of a constant inversion lid at 300 meters, but merely serves as an artifice to adjust the calculation.) Correction factors as a function of distance between infinite and finite mixing depths are given in Figure 2-4 for a typical sector.

The current meteorological data acquisition program has been updated to permit azimuth and elevation angle standard deviations to be calculated from direct measurements, rather than depending on correlation and classification techniques.

Table 2-I. Classification of Atmospheric Stability

Stability Classification	ΔT/ΔZ, °C/100m	Pasquill Categories	BNL Categories
Extremely Unstable	<-1.9	A	Unstable
Moderately Unstable	-1.9 to -1.7	B	"
Slightly Unstable	-1.7 to -1.5	C	"
Neutral	-1.5 to -0.5	D	"
Slightly Stable	-0.5 to 1.5	E	Stable
Moderately Stable	1.5 to 4.0	F	"
Extremely Stable	>4.0	G[a]	"

a. No graphical data available for G. This category was treated as F.

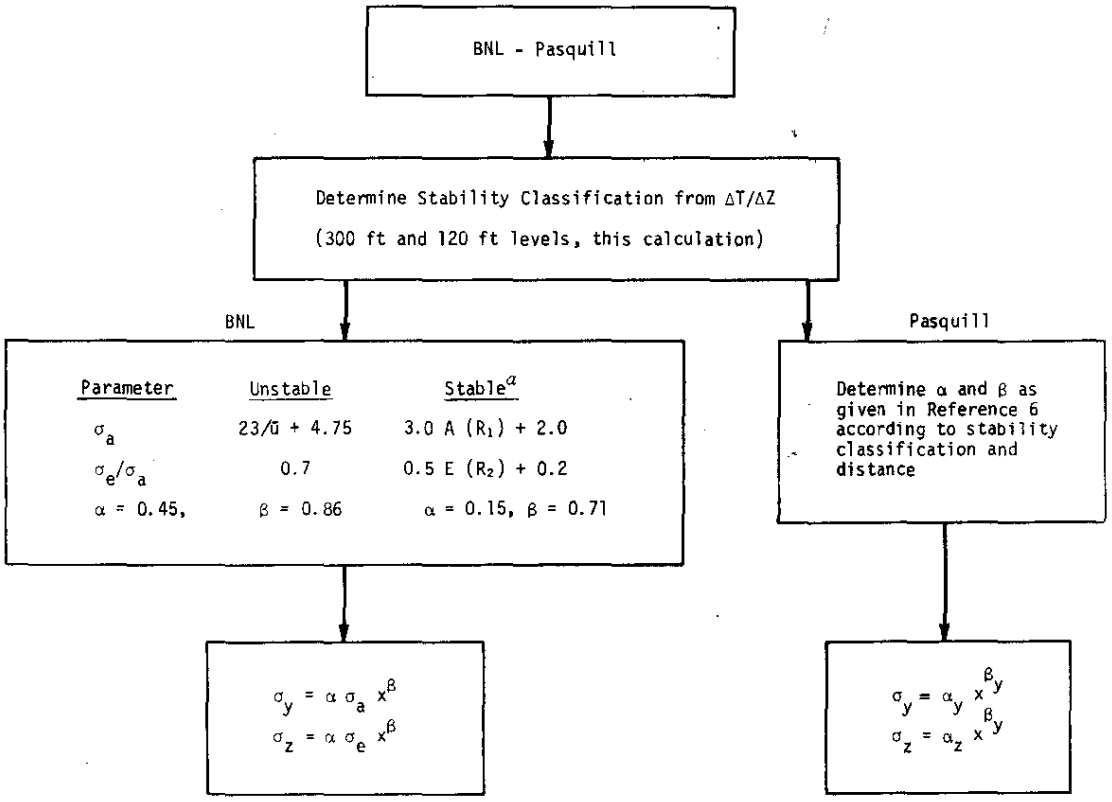

a. A (R_1) and E (R_2) are random numbers generated independently and uniformly distributed between 0.0 and 1.0.

Figure 2-1. Dispersion Parameter Derivation

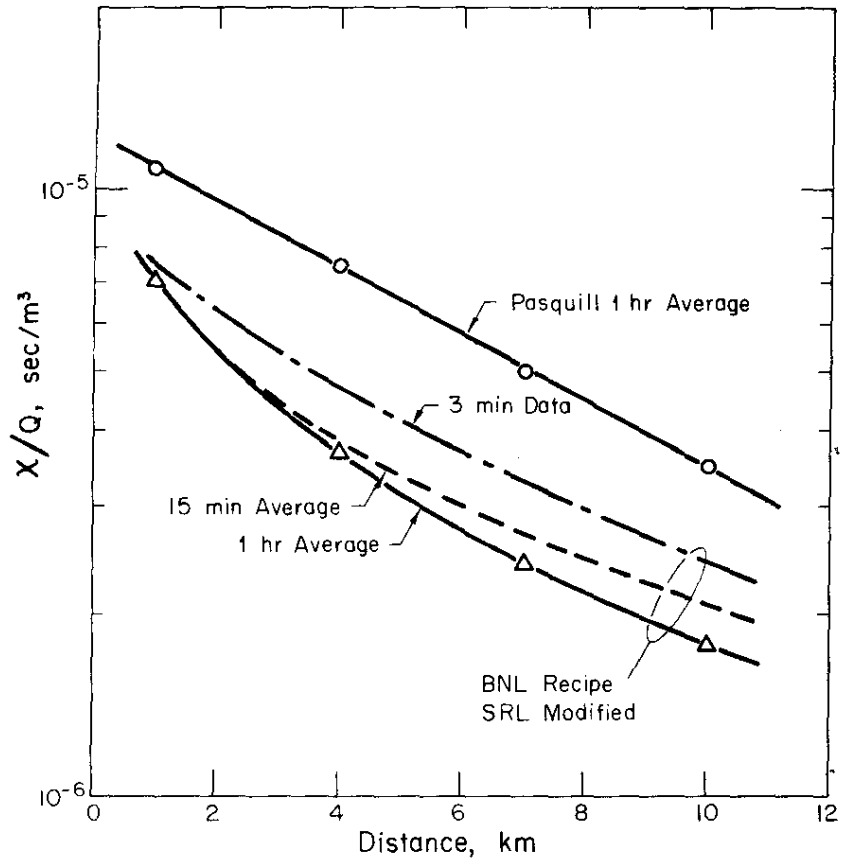

Figure 2-2. Calculations of Surface χ/Q at the 95th Percentile Derived from SRL Meteorological Data and an Assumed 65m Release Height

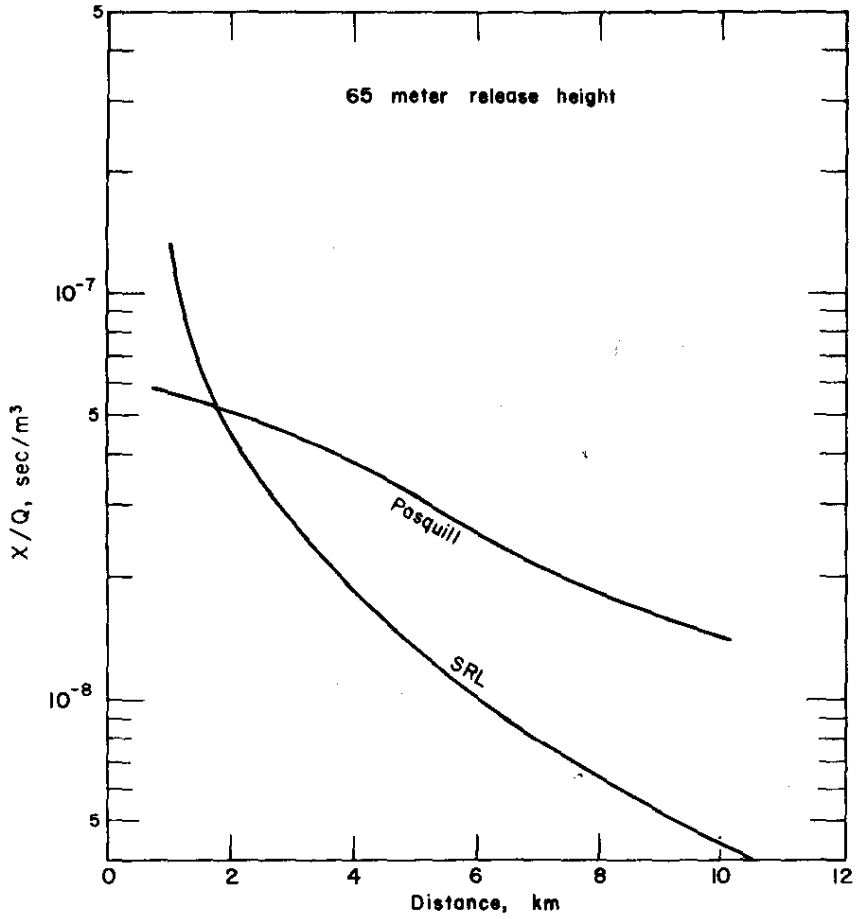

Figure 2-3. Annual Average χ/Q (Azimuthally Averaged)

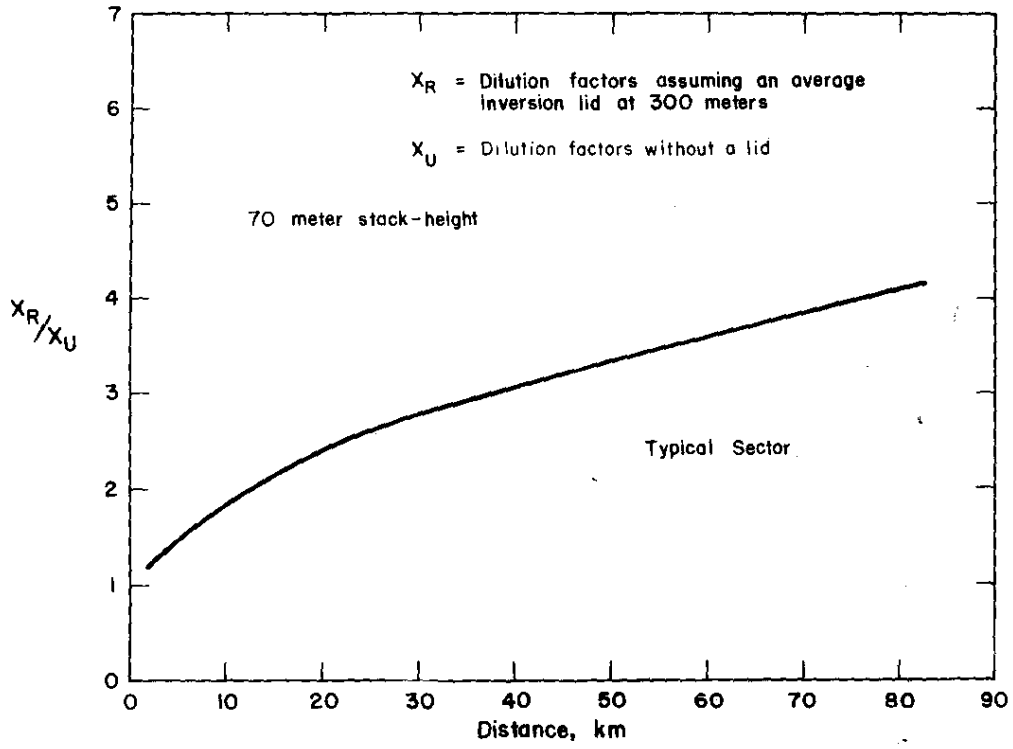

Figure 2-4. Ratio of Yearly Averaged Dilution Factors at Ground Elevation.

REFERENCES

1. I. A. Singer, J. A. Frizzola, and M. W. Smith. "Simplified Method of Estimating Atmospheric Diffusion Parameters." *J. Air Pollution Control Assoc. 16 (11)*, 594-596 (1966).

2. *Safety Guides for Water Cooled Nuclear Power Plants.* Division of Reactor Standards, USAEC, Safety Guide 23 (Feb. 1972).

3. F. Pasquill. "The Estimation of the Dispersion of Windborne Material." *Meteorol. Mag. 90* 1063 (1961).

4. R. E. Cooper and B. C. Rusche. *The SRL Meteorological Program and Off-Site Dose Calculations.* USAEC Report DP-1163, Savannah River Laboratory, E. I. du Pont de Nemours and Co., Aiken, S. C. (1968).

5. F. A. Gifford. "Use of Routine Meteorological Observations for Estimating Atmospheric Dispersion." *Nuclear Safety 2(4)*, 47-51 (1960).

6. J. Tadmor and Y. Gur. "Analytical Expressions for the Vertical and Lateral Dispersion Coefficients in Atmospheric Diffusion." *Atmos. Env., 3*, 688-689 (1969).

3. METEOROLOGICAL DATA FROM THE WJBF-TV TOWER†

INTRODUCTION

During May 1973, a new data acquisition system *(Datacom)* became operational at the WJBF-TV tower near Beech Island, S. C. The *Datacom* magnetic tape recorder system* replaced the paper tape recorder system installed by SRL to collect meteorological data during the period 1966-1972. The following is a description of the data format of the new system and the codes used for data processing and quality control.

DATA ACQUISITION

The *Datacom* acquisition system currently has the capability of monitoring and recording 32 channels of data. Variables routinely monitored as of July 1973 are wind speed, wind direction, and temperature at seven different elevations ranging between 2 and 330 meters. In addition, two references voltages are recorded to monitor the system operation. All data are recorded on magnetic tape in blocks, each consisting of a prescribed number of complete data scans (currently 11 scans per block). Each data scan (or record) is preceded by a notation of the year, day, hour, minute, and second. The data acquisition system has the capability of scanning all 32 channels at a wide range of frequencies up to and exceeding the response capabilities of the sensors in use.

The data are written on tape in a format compatible with SRL's *IBM 360/195*** system. At a scanning rate of one cycle per 5 seconds (36 words), a 2400 foot reel of magnetic tape can record about 10 days of data. These tapes are subsequently processed with the *IBM 360/195* system to convert the data to engineering units and to reblock the data into a more compact format. As a result of campacting, the permanent system labeled tapes will hold about 80% more data than the tapes originally written by the *Datacom* acquisition system.

---

† Work done by M. M. Pendergast and R. E. Cooper

* Product of Datacom, Inc., Fort Walton Beach, Florida.

** Product of International Business Machines, Armonk, New York.

NECESSITY FOR QUALITY CONTROL

Several factors make it imperative that quality control be maintained on the meteorological data collected at the WJBF-TV tower. They are:

1. Output from the seven *Climet* Bi-Vane Wind Sensors and the seven temperature sensors are collected on magnetic tape only; no hard copies or strip charts are recorded simultaneously. It is important that these data be inspected periodically for errors that could be caused by instrument, tower wiring, or recorder malfunction.

2. Meteorological data from TV towers at other sites have been collected using the more-rugged *Aerovane** wind system. As one of the purposes of the WJBF-TV tower system is to collect meaningful turbulence data at low wind speeds, instruments more sensitive than the *Aerovane* system are required. These more-sensitive instruments, such as the *Climet* Bi-Vane, are much more difficult to keep operating continuously.

3. These data are to be used for dose calculations from routine releases and for various safety analysis studies. For this purpose, a data recovery rate of 90 percent is desirable; consequently, a quality control program is a necessity.

4. The TV tower data and data from the seven area towers will eventually be incorporated into an improved forecast capability for quick response to emergencies.

Usually, major system malfunctions are obvious. The challenge is an early detection of such things as an intermittent wiper contact in one of the wind direction units, a burned-out bulb in an anemometer, a bent bivane tail, etc.

The most desirable quality control program would be one designed to examine the data for physical consistency as it is stored on the *Datacom* tape unit. Such a sophisticated procedure, though possible, is not practical at this time. A more practical quality control program combines data collection with compressing the data onto another tape. A periodic check of the data is currently being done at a frequency of at least once per week.

---

* Product of Bendix Corp., Baltimore, Maryland.

QUALITY CONTROL

The simplest and most-direct approach to quality control is to examine the data for physical consistency by plotting the temperature and wind data as a function of height. The data are plotted four times for each day to sample different stability conditions. Mean values of approximate potential temperature (given by the sum of the temperatures at level Z and $\gamma_d Z$, where γ_d is adiabatic-lapse rate), horizontal wind direction, vertical wind direction, and wind speed are calculated for a 60-minute period centered on the four major synoptic time periods (0000, 0600, 1200, and 1800 GMT*). As the standard deviation is more sensitive to a single erroneous piece of data, this parameter is also calculated with each mean value.

A sample of the computer plot for Day 172 at 2300 EST** is shown in Figure 3-1. Mean values of each parameter are plotted against the logarithm of height and are connected with straight lines to show the variation with height. Points corresponding to plus and minus one standard deviation unit from the mean are indicated with O's at each level. The horizontal line connectiong the O's thus represents the limits containing 67% of the observations. Unrealistic values of the parameters caused by short circuits are indicated with U's plotted at their respective levels.

The wind speed profile indicated in the upper left plot of Figure 3-1 closely fits a straight line. This fit implies that the wind speed increase with height closely follows the log law for a near-surface neutral condition over the entire height of the TV tower at this particular hour. As the sample was taken during a cloudy evening of high wind speeds, neutral conditions prevailed, and the expected log law wind profile applies. Note, however, the plot of horizontal wind direction on the lower left plot of Figure 3-1. The 200-meter direction shows a marked contrast to the directions immediately above or below this level. Since no sharp contrast occurs in the wind speed profile, this direction is probably in error. Thus, examination of data presented in this format does permit judgments to be made on the physical reasonableness of the data. Comparisons can be made with time as well as height to see if a particular suspicious feature exists with time. Note also that the standard deviations of horizontal and vertical wind direction show a marked decrease with increasing elevation. For this example, the observed decrease is probably caused by the inverse relationship between wind variability and wind speed.

---

*Greenwich Mean Time

**Eastern Standard Time

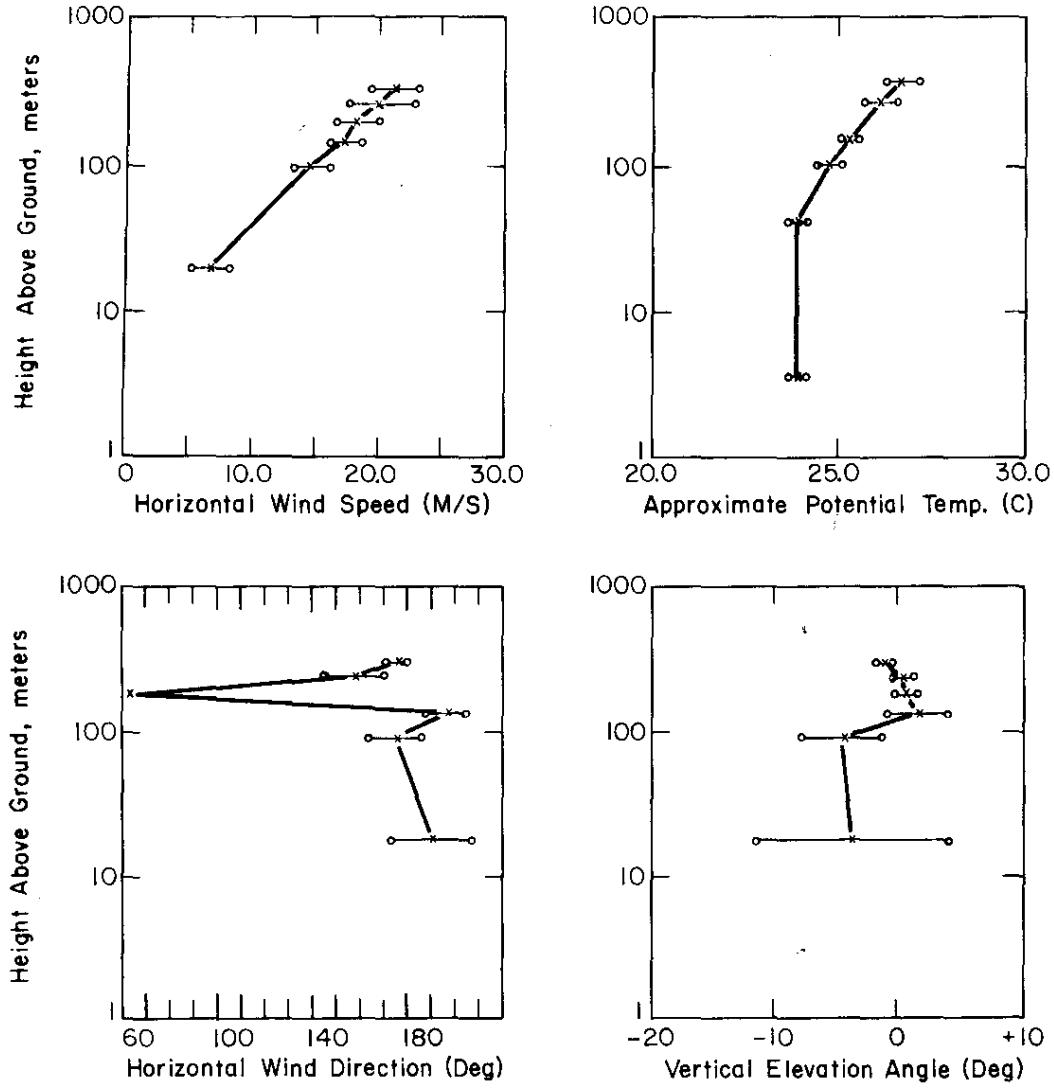

WJBF-TV TOWER DATA: DAY 172 TIME PERIOD 2234-2334 SAMPLE RATE (SEC) 5.0 N=720 RI=0.043

Z (m)	Speed (m/s)			Hor Dir (Deg)			Vert Dir (Deg)			P (Power Law)	
	AVE	SD	P-P/SD	AVE	SD	P-P/SD	AVE	SD	P-P/SD	Temp	Speed
18.2	6.91	1.31	6.61	188.0	15.83	5.55	56.2	7.52	6.87	00	0.45
31.4	4.66	1.17	5.52	164.0	9.66	5.05	55.3	2.79	8.97	0.02	0.40
137.2	7.29	1.87	4.81	187.0	5.40	6.10	61.3	2.23	1.15	0.05	0.18
182.9	8.21	1.48	4.21	56.0	1.97	5.57	60.3	0.53	6.51	0.05	0.34
243.8	8.12	2.37	3.44	146.0	10.80	5.83	60.2	0.40	5.38	0.07	0.23
384.8	1.23	1.73	4.33	164.0	3.24	6.46	99.5	0.00	9.90 AVE	0.04	0.32

Figure 3-1. An Example of the Computer Printout Used to Maintain Quality Control of Meteorological Data from the WJBF-TV Tower.

The table at the bottom of Figure 3-1 summarizes some of the information displayed on the plots. This table also provides additional information to help describe the conditions prevailing during the time period represented by the plot. In general, the following information is contained in the table:

1. Sampling time, to validate the time period represented by the plots.

2. Sampling rate and the number of points used to calculate statistics.

3. The Richardson number R_i, where $R_i = (g/\theta)(\partial\theta/\partial Z)/(\partial\bar{v}/\partial Z)^2$ evaluated within the 20 to 100 m layer, and θ = potential temperature, g = acceleration due to gravity, Z = height, and $\bar{v}$ is average wind vector.

4. Average and standard deviations of wind speed, horizontal wind direction, and vertical elevation angle at each level.

5. The quotient determined by dividing the observed range of the variable by its calculated standard deviation.

6. The exponent of the relationships,

$$\theta = \theta_o(Z/Z_o)^{P\theta} \text{ and } V = V_o(Z/Z_o)^{Ps}$$

to describe the profiles of potential temperature and wind speed, respectively, between successive levels and also the arithmetic average of these values for all levels.

An analysis of these plots and tables will be instructive and will improve quality control. A catalog of the computer printouts will be available as a ready reference to meteorological data collected and stored at SRL.

4. MESOSCALE SPECTRAL STUDIES OF WIND DATA FROM A 1200-FOOT TV TOWER†

INTRODUCTION

The turbulent dispersion characteristics of the atmosphere must be calculated to estimate the dispersion of pollutants released into the atmosphere. The problem is complex, as the atmosphere is in a constant state of change and is characterized by turbulent eddies of various sizes. In a statistical sense, probably the simplest representation of the turbulent state of the atmosphere is through the use of kinetic energy spectra. Kinetic energy spectra display turbulent fluctuations of the wind as a function of the period (wavelength or wavenumber) of the turbulence. Figure 4-1 shows an idealized spectrum[1] depicting the distribution of atmospheric kinetic energy over a wide range of scales corresponding to periods between 1 month and 1 second.

Most kinetic energy is found centered around two peaks: the first, at a period of 4 days, and the second, at a period of 2 minutes. The 4-day peak is associated with synoptic scale weather systems. These motions are considered to be quasihorizontal since the wavelengths involved, several thousand kilometers, are large compared with the depth of the weather-producing atmosphere, 10 km.

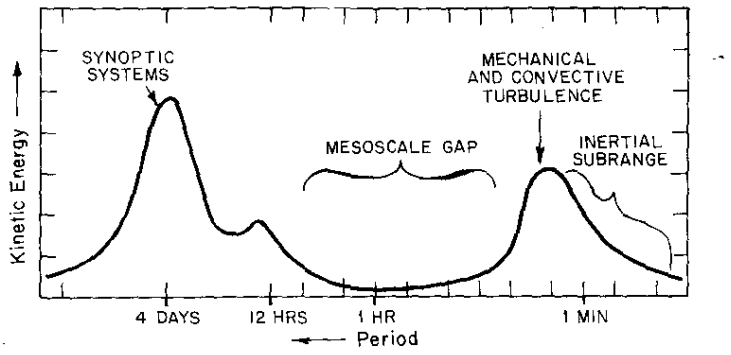

Figure 4-1. An Idealized Representation of Kinetic Energy Available at Different Wavelengths (after Van der Hoven[1]).

† Work done by M. M. Pendergast and T. V. Crawford

The 2-minute peak is usually associated with mechanical and convective turbulence. Mechanical turbulence is produced as the result of surface roughness and wind shear. Convective turbulence is produced as the result of buoyant motions caused by variations in the vertical temperature gradient. Eddies produced by both mechanisms are of the same general size.

The kinetic energy available between these two peaks is generally much smaller. This "gap" in kinetic energy is called the mesoscale gap because of its appearance at wavelengths typical of the mesoscale. It is thought that the mesoscale gap primarily occurs because of one of the following reasons.[2]

1. Kinetic energy is lost over this frequency band at a rate faster than viscous dissipation. A primary example of a mechanism to achieve this is an air parcel working against gravity.

2. An input of kinetic energy at either side of the mesoscale gap. These inputs could be of the form of diurnal fluctuations of wind speed (e.g., from a low level jet stream) or of mechanical turbulence caused by wind shear and ground roughness.

The similarity theory as developed by Kolmogoroff[3] provides a means to predict the shape of the kinetic energy spectra over certain frequency ranges. The fundamental concept of the theory is that turbulent motion is characterized by a wide range of scale sizes and that energy is continually passing from large to small scales. Ultimately a limit is reached when the kinetic energy produces only heat in the random motion at a scale size where molecular viscosity is important.

Kolmogoroff[3] defines an inertial subrange over which the eddies are much smaller than those of kinetic energy input and much larger than those associated with viscous dissipation. Over this subrange, the average properties of turbulence are determined uniquely by the average rate of dissipation of energy per unit mass of the fluid. Dimensional analysis yields diffusion predictions within the inertia subrange.

Under many situations, the gap in the kinetic energy spectra exists between periods of 1 minute to 12 hours.[1] Measurements have also been made[2] that suggest that during particular synoptic conditions and over certain terrain features this mesoscale gap does not exist.

The following sections will show the effect of a mesoscale gap on the diffusion of a hypothetical puff. The shapes of kinetic energy spectra are shown at mesoscale wavelengths using

data collected over a two year period (1966-1968) at the instrumented TV tower near SRP.

KINETIC ENERGY SPECTRA AND ATMOSPHERIC DIFFUSION

Similarity theory is helpful to show the relationship between the diffusion of a hypothetical puff and the kinetic energy spectra applicable at the time of the release of the puff. The increase in horizontal area of a hypothetical puff emitted under conditions represented by two different spectra are examined. Inherent in this examination is the assumption that the puff will be dispersed most efficiently by atmospheric motions having the same size as the puff, implying that atmospheric motions with scales much smaller than the puff will cause the puff to expand only slightly. Atmospheric motion with scales larger than the puff will cause the puff to be translated rather than be diffused.

The spectra for the comparison are constructed in such a way that the energy distribution with wavelength follows that given by the similarity theory. Thus, the following relationships show the rate of increase of the hypothetical puff with time.[4]

$$S(n) = a\left(\frac{n}{\bar{u}}\right)^{-5/3} \cdot \left(\varepsilon\right)^{2/3}, \quad a = 0.5 \tag{1}$$

$$\sigma_t^2 = \sigma_o^2 + \varepsilon t^3 \tag{2}$$

Equation 1 shows that the kinetic energy S(n) at frequency n is a function of the mean wind speed ($\bar{u}$) and the dissipation rate (ε). Equation 2 indicates that the size of a puff (σ_t^2)* is a function of its initial size (σ_o^2), the dissipation rate (ε), and the elapsed time (t).

Figure 4-2 shows spectra for two different synoptic conditions with energy represented on the ordinate and wavelength represented on the abscissa. Note that the spectra follow the -5/3 law for all wavelengths, but that the magnitude of the energy changes with different values of ε. Spectrum A assumes the dissipation is constant for all wavelengths between 10 meters and 3000 kilometers. This spectrum also assumes the inertial subrange extends through the synoptic scale for horizontal motions, as observed by several investigators.[2,4]

---

* σ_t^2 represents the variance of the mean separation distance between two particles within the puff. We assume that one is the center of the puff. Thus, σ_t represents the radius of the puff (as defined) and 67% of the particle are within this radius.

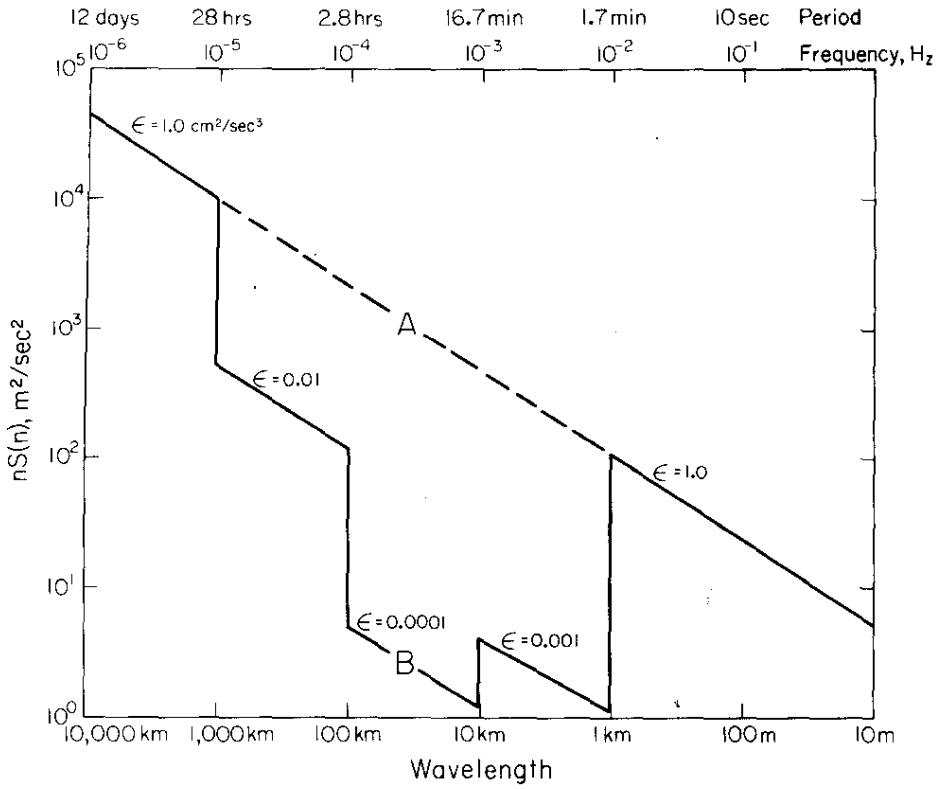

FIGURE 4-2. Kinetic Energy Spectra for Two Different Atmospheric Conditions Each Having a Mean Wind Speed of 10 m/s.

Spectrum B (Figure 4-2), although assumed to follow similarity theory predictions at all wavelengths, reproduces a mesoscale gap by assuming that the magnitude of the dissipation rate is a function of wavelength. Although a crude approximation, the spectrum constructed by this means generally fits many observed spectra for which a mesoscale gap exists. The values of ε (used to define the mesoscale gap) are of the same order of magnitude as values calculated using Equation 1 and spectra calculated from WJBF data. Thus, Spectrum B is representative of spectra observed at SRP.

Figure 4-3 shows a comparison between the rates of expansion of a hypothetical puff with and without a mesoscale gap. The rates of expansion are consistent with the kinetic energy of spectra A and B (Equation 2). The abscissa represents the elapsed time from the release of the puff (in seconds), and the ordinate represents the variance of the mean separation distance of two particles within the puff. Both puffs were assumed to be released at time zero, and both puffs had an initial horizontal size (area$=\pi\sigma_0^2$) of 10^8 cm^2.

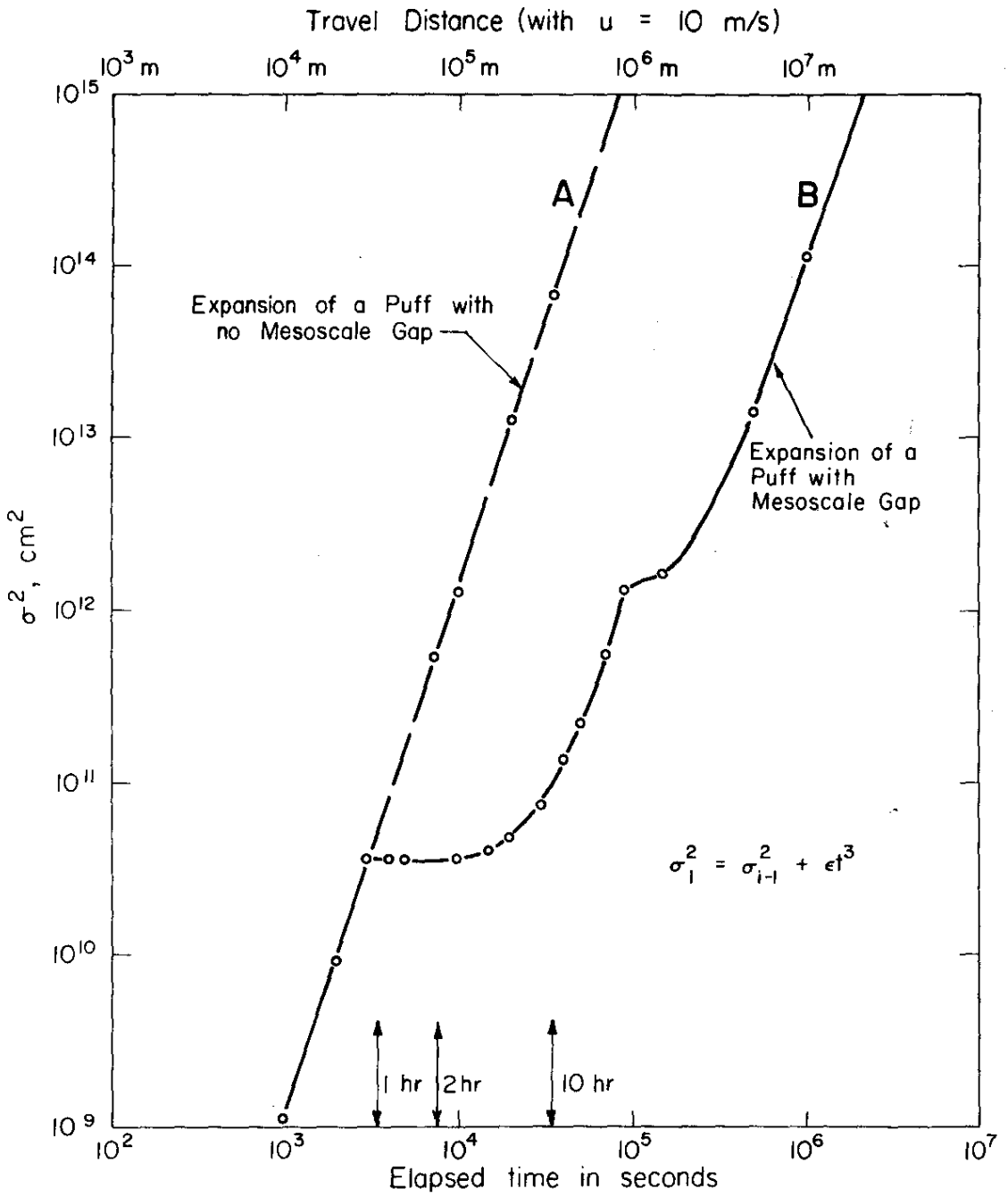

Figure 4-3. A Comparison of the Rate of Increase of a Hypothetical Puff Released Under Influence of Atmospheric Conditions Described by the Kinetic Energy Spectra of Figure 4-2.

At an elapsed time of one hour, there is virtually no difference between the two puffs. At an elapsed time of two hours, however, the puff released in atmospheric conditions associated with Spectrum B is almost tenfold smaller than the puff associated with Spectrum A. At an elapsed time of ten hours, the puff associated with Spectrum B is almost 1000 times smaller than the puff associated with Spectrum A. The pollutant concentration within the puff is inversely proportional to the puff area; therefore the resulting concentration after a travel time of ten hours for the puff associated with Spectrum B would be one thousand times larger than the concentration of the puff associated with Spectrum A.

KINETIC ENERGY SPECTRA AT SRP

Kinetic energy spectra with periods of 0.5 to 20 hours were interpreted with one primary goal in mind: to determine if (or when) similarity theory predictions are valid at SRP. Spectra of wind data obtained from a TV tower located near Beech Island, S. C., during 1966-1968 have been analyzed. The data were obtained at 6 levels between 120- and 1000-ft above ground level. A total of 15 cases representing different time series of wind data averaged over 15-minute periods were available for study. These case studies had sampling periods ranging between 6 and 10 days.

Energy spectra were computed using an autocorrelation function procedure,[5] and the estimates were smoothed by the "hanning" technique. The sample size, N, varied between 576 and 960 for the 15 cases studied. Blackman and Tukey[5] suggest the number of lags (m) used should be chosen according to sample size so that the degrees of freedom (F) given by

$$F = \frac{2\left(N - \frac{m}{4}\right)}{m} \qquad (3)$$

is greater than 30. For N = 576 and F = 30, an upper limit on the number of lags used is about 40.

With this lag and with the time between points (dt) of 15 minutes, the range of frequencies covered was between n_1 (=1/2m dt) and n_2 (= 1/2 dt). This range corresponded to frequencies between 0.05 and 2.00 cycles/hour or periods from 20 hours to 1/2 hour.

COMPOSITE SPECTRA

To examine the general applicability of similarity theory to the SRP area, spectral estimates for all 15 cases were grouped together. The 15 cases are distributed seasonally, with 4 cases each in winter, fall, and summer, and 3 cases in spring. Thus, the range of the values of the spectral estimates is assumed to be representative of the range one would expect to find from seasonal changes.

Spectra estimates normalized by variance for 6 levels on the WJBF-TV tower are shown on Figures 4-4 and 4-5. The diagonal lines represent the -5/3 law predicted by the similarity theory. Several general conclusions can be drawn from the two figures:

1. Spectra estimates for the levels above 300 ft appear to fit a -2 law [slope $\sim$ -1 on a plot of nS(n) versus n].

2. Spectra estimates for the 300-ft level appear to fit a -5/3 law [slope $\sim$ -2/3 in a plot of nS(n) versus n].

3. Spectral estimates for the 120-ft level appear to fit a -4/3 law [slope $\sim$ -1/3 on a plot of nS(n) versus n].

The fairly smooth transition from a slope of -1 at the upper levels to -1/3 at the 120-ft level apparently results from a decrease of energy at the low frequency end of the spectrum and an increase in energy in the high frequency portion as the ground is approached. The kinetic energy at the high frequencies is produced mechanically by a) surface roughness and/or wind shear, and b) buoyant motions caused by hydrostatic instability. At high frequencies, both factors tend to become less significant as distance from the ground increases. Thus, more energy can be expected to be available in the high frequency end of the spectrum at the lower levels.

The variation of kinetic energy with height at the lower frequencies is not so easily understood. Conceptually, energy is cascaded from the synoptic scale down to the microscale. Superimposed on this process is a mesoscale input of energy. These sources of kinetic energy include systems with strong diurnal variations, such as sea breezes, mountain-valley flow, and the low-level jet. Also included are frontal structures, squall lines, and long gravity-waves,[6] all of which could contribute to energy added at the mesoscale frequencies. In addition, wind speed normally increases with increasing height, so the average contribution to kinetic energy at these frequencies will increase with height, independent of the particular mesoscale mechanism producing the energy.

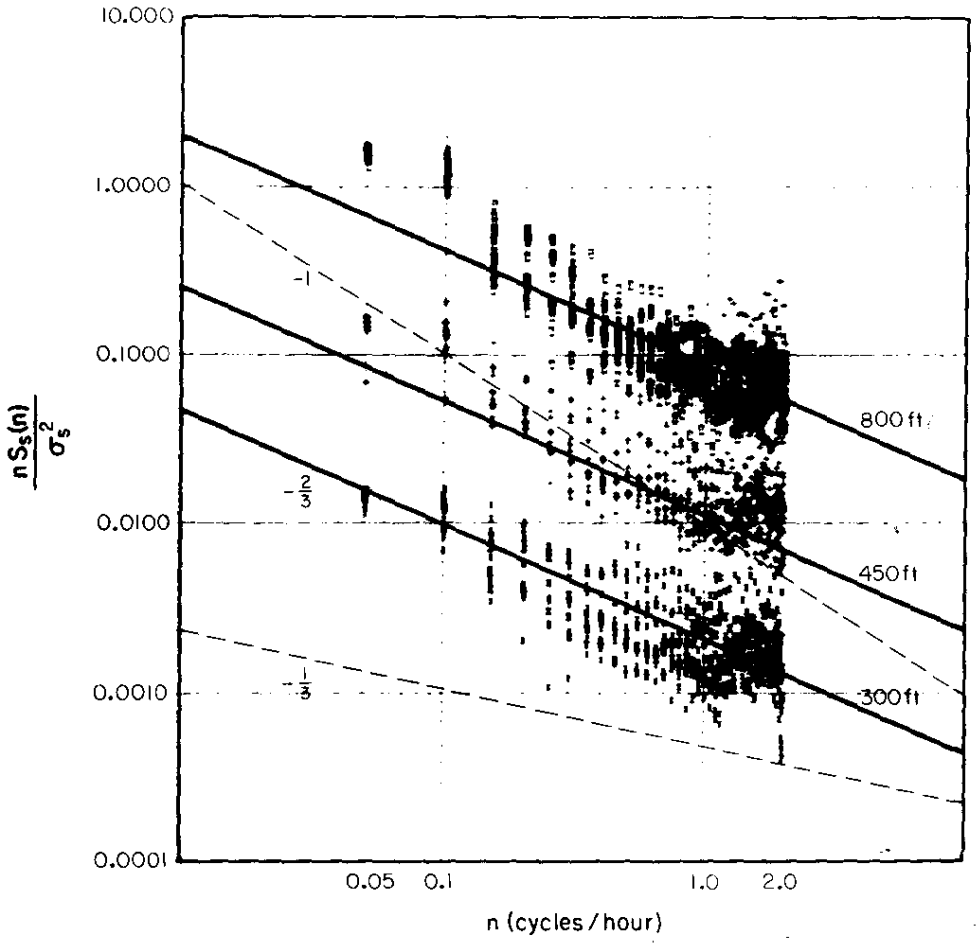

FIGURE 4-4. Kinetic Energy Spectra Normalized (by Variance) of Scalar Wind Speed for 3 Levels on the WJBF-TV Tower for All 15 Cases. Spectral Estimates for the 300-ft Level are Indicated by x. Spectral Estimates for the 450-ft Level Multiplied by 10 Are Represented by +. Spectral Estimates for the 800-ft Level Multiplied by 100 Are Represented by 0.

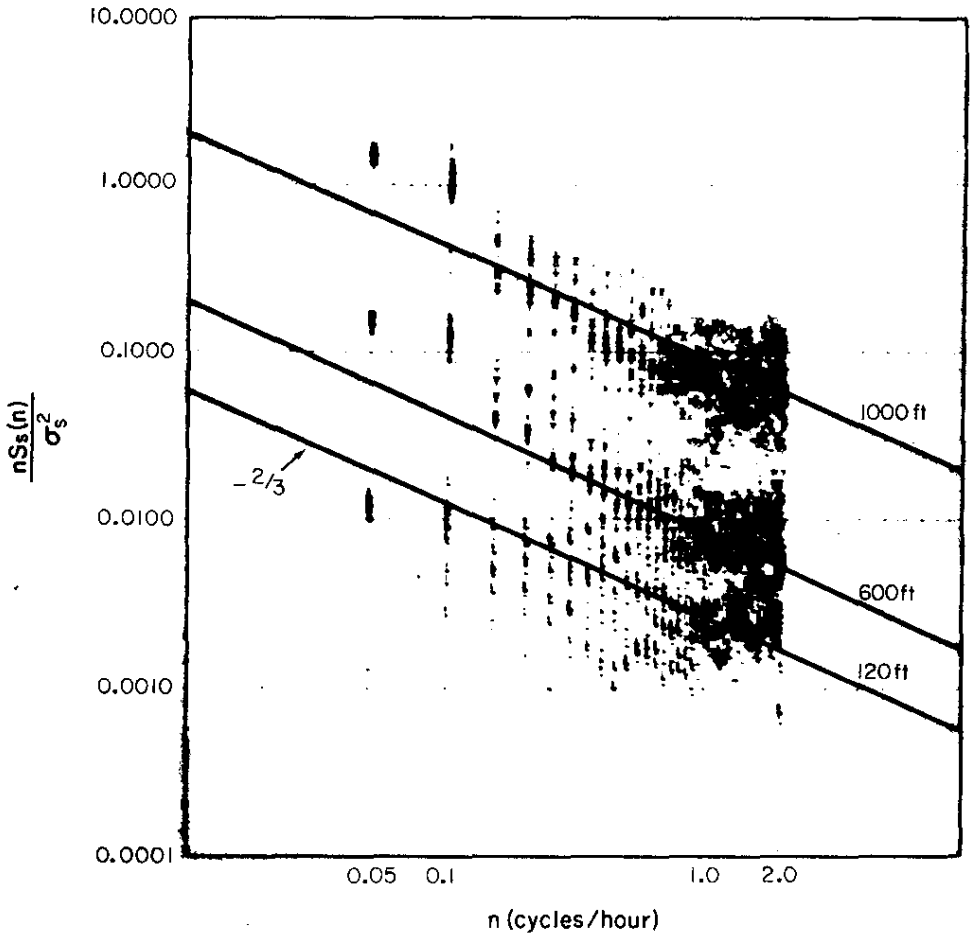

FIGURE 4-5. Kinetic Energy Spectra Normalized (by Variance) of Scalar Wind Speed for 3 Levels on the WJBF-TV Tower for All 15 Cases. Spectral Estimates for the 120-ft Level Are Indicated by L. Spectral Estimates for the 600-ft Level Multiplied by 10 Are Represented by Y. Spectral Estimates for the 1000-ft Level Multiplied by 100 Are Represented by x.

From the above reasoning, it is logical to assume that at an intermediate level the distribution of kinetic energy with frequency will fall along the predicted (-5/3 law) line. The composite spectra indicate that this level is located between 120 and 300 ft. As most SRP effluents are released from 200-ft-high stacks, similarity theory predictions may not be too unreasonable at SRP.

SPECTRA FOR THE PERIOD FEBRUARY 15 - MARCH 12, 1967

Three of the original 15 case studies were separated by brief (2-hour) periods containing no data. A time series was made up of the three above series with the missing data filled in by linear interpolation. The increased sample size and increased number of lags (400) permit a more detailed investigation of the relationship of the energy available between the macroscale and the mesoscale.

With respect to synoptic weather conditions, this period represents an abnormal late-winter situation with several Arctic fronts pushing into South Carolina. Generally, frontal passages were occurring at intervals of 3 days. Temperatures showed wide variations during this period with below-freezing temperatures associated with Arctic air masses and warm temperatures associated with maritime tropical influences.

From the variations in the synoptic pattern, one would expect the time series of wind data to include variations attributed to synoptic scale motions. To depict the energies at these periods, spectral estimates were obtained between periods of 8 days and 1/2 hour. The wind statistics at 6 levels on the WJBF-TV tower are presented in Table 4-I.

TABLE 4-I. Wind Statistics for February 15 - March 12, 1967

Speeds ($\bar{u}$, $\bar{v}$, $\bar{s}$, $\bar{w}$), m/s; variance (σ^2), m^2/sec^2

Level, ft	East-West		North-South		Scalar		Vertical	
	$\bar{u}$	σ^2_u	$\bar{v}$	σ^2_v	$\bar{s}$	σ^2_s	$\bar{w}$	σ^2_w
120	2.0	12.9	1.5	9.9	4.9	5.0	-0.5[a]	0.3
300	2.7	19.7	1.9	17.8	6.4	7.7	-0.6	0.4
450	3.4	27.5	1.9	24.0	7.5	10.4	-0.7	0.6
600	4.0	33.6	2.1	28.2	8.3	13.3	missing	
800	5.1	33.9	-0.5	34.1	8.8	16.6	missing	
1000	4.5	32.1	2.2	31.4	8.3	18.8	missing	

a. $\bar{w}_{120} = \phi_{300} \cdot s_{120}$

Generally, the average wind direction veers with increasing height (clockwise turning) ranging from SW at 120 ft to WNW at 800 ft. Accompanying the wind direction change with height is an increase of scalar wind speed; the lowest speeds occur at the 120-ft level, and the highest speeds occur at the 800-ft level. The variance of the scalar wind speed increases from 5 m^2/s^2 at 120 ft to 18.8 m^2/s^2 at 1000 ft. The variance of the component wind speeds indicates a similar increase with height, with values generally twice the values of the variance of the scalar wind speed at each height. The variance of the components at each height are almost equal.

Spectra of Scalar Wind Speed

Figure 4-6 shows the distribution of kinetic energy with frequency for six levels on the WJBF-TV tower. The most prominent features of the spectra are the peaks which correspond to periods of three days and one day.

The 3-day peak, corresponding to large scale synoptic influences, is present at all levels, with more energy at the higher levels. The 1-day peak associated with the diurnal changes in wind velocity is pronounced on all spectra except for the 120-ft level. In general, the kinetic energy available at this frequency increases up to the 600-ft level and is fairly constant above 600 ft.

The kinetic energy decreases with increasing frequency. The rate of decrease is highest at levels above 450 ft and lowest at the 120-ft level.

Spectra of North-South Components

The v-spectra for all levels (Figure 4-7) show peaks associated with synoptic and diurnal frequencies. In addition, all levels show a peak near 3.0×10^{-5} Hz, corresponding to a period of about 10 hours. As in the case for the 3-day and 1-day peaks in the spectra of scalar wind speeds, the energy associated with the semi-diurnal variation (1/2-day peak) appears to increase with increasing height. The existence of semi-diurnal peaks in the u-component spectra without such peaks showing on the scalar wind speed spectra is possibly caused by directional changes as described by Wendell[7] for Idaho Falls, Idaho.

Spectra of East-West Components

In general, the conclusions for the v-spectra are applicable to the u-spectra (Figure 4-8). No clear-cut wind direction prevails throughout the period which could cause one of the components

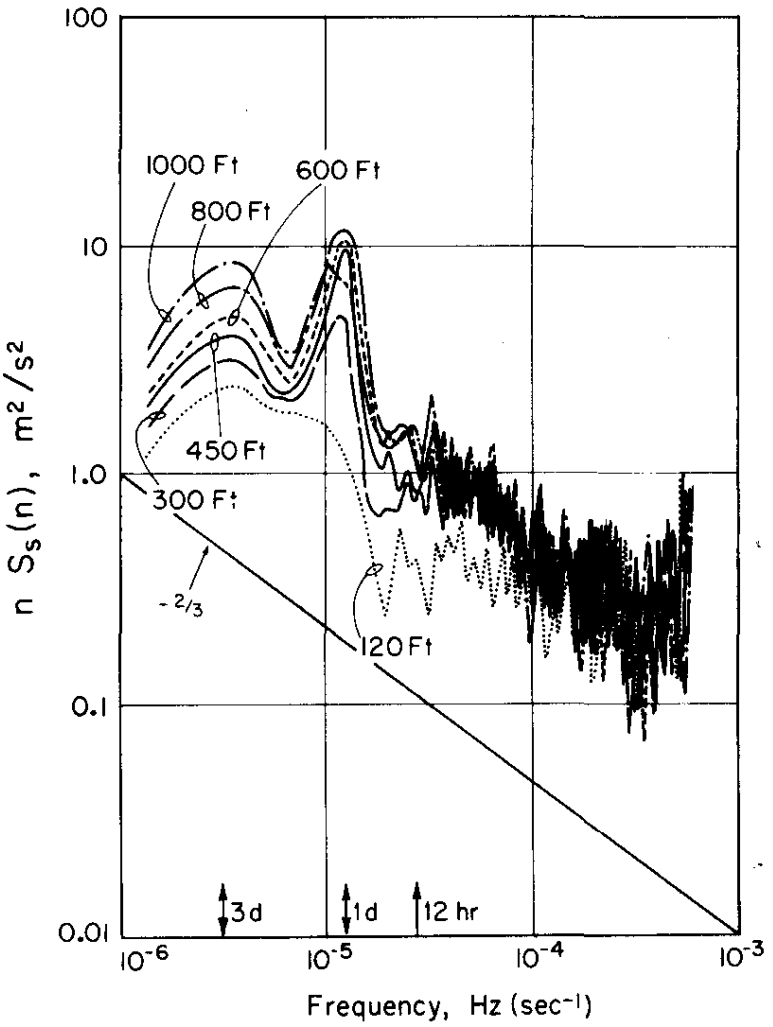

Figure 4-6. Kinetic Energy Spectra of Scalar Wind Speed, $\bar{s}$.

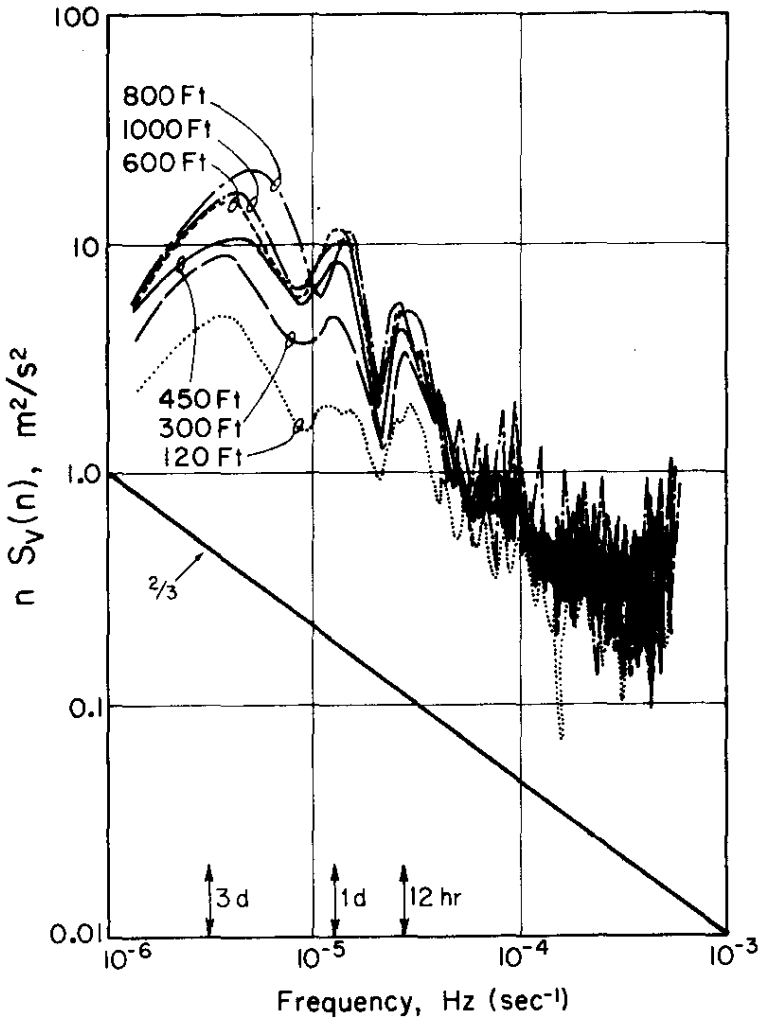

Figure 4-7. Kinetic Energy Spectra of North-South Component, $\bar{v}$.

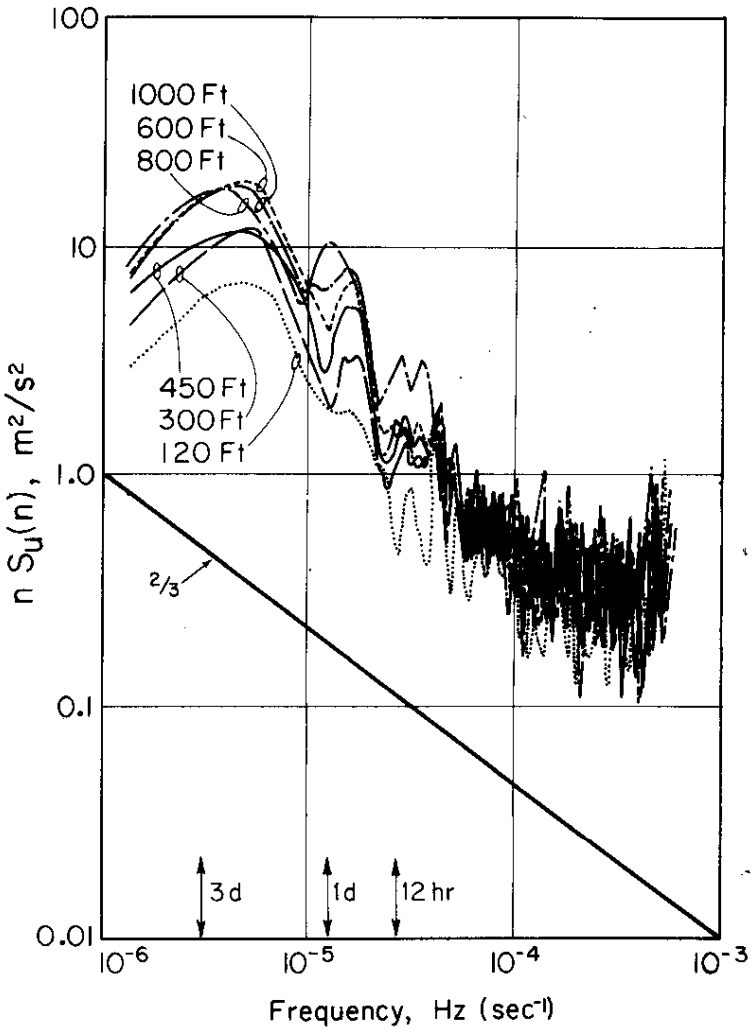

Figure 4-8. Kinetic Energy Spectra of East-West Component, $\bar{u}$.

to approximate the transverse components and the other to act similar to the longitudinal components.

Some aspects of the u-spectra are different from the v-spectra. The most pronounced difference is the absence of the semi-diurnal peaks on the u-spectra at all levels except at the 800-ft level. Also noticeable are the smaller diurnal peaks at the 120-ft level.

Spectra of the Vertical Component

The spectra of the vertical wind speed for only three levels on the WJBF-TV tower are shown in Figure 4-9 because instrument failures occurred during a significant portion of the sample period. The most important aspect of these spectra is the fact that the energy associated with the lower frequencies is almost 100 times smaller than for the horizontal spectra.

The energies associated with the higher frequencies for the vertical component are of the same magnitudes as the energies for the horizontal components, which indicates isotropy at high frequencies (1/2 hour in this study). Noticeable are gaps in the energy spectra centered near the semi-diurnal frequency. An increase in energy associated with synoptic and diurnal frequencies at increasing altitudes is depicted, producing stronger mesoscale gaps at the higher levels.

SUMMARY OF FEBRUARY 15 - MARCH 12, 1967 SPECTRA

In general, the kinetic energy spectra for February 15 - March 12, 1967, show three major peaks. The largest major peak is associated with synoptic scale motions having a period of 3 days. For most levels, more energy is associated with the components than with the scalar speed spectra. This observation leads to the conclusion that most velocity fluctuations associated with synoptic changes are in the wind direction.

The second largest major peak is associated with the diurnal cycle having a period of one day. At the 120-ft level, the diurnal peaks are most evident in the v-spectra indicating directional influences are important. For higher levels, the peak shows up in all three spectra, the largest energies being associated with the four highest levels. This conclusion agrees with results obtained concerning the diurnal variation in dispersion discussed by Pendergast in Section 6. The diurnal peaks for the u and v component spectra are about the same magnitude as the scalar speed spectra, indicating the importance of wind speed to the diurnal peaks. The diurnal peaks for the components are smaller than the corresponding synoptic peaks implying less dependence on wind direction fluctuation for the diurnal peaks.

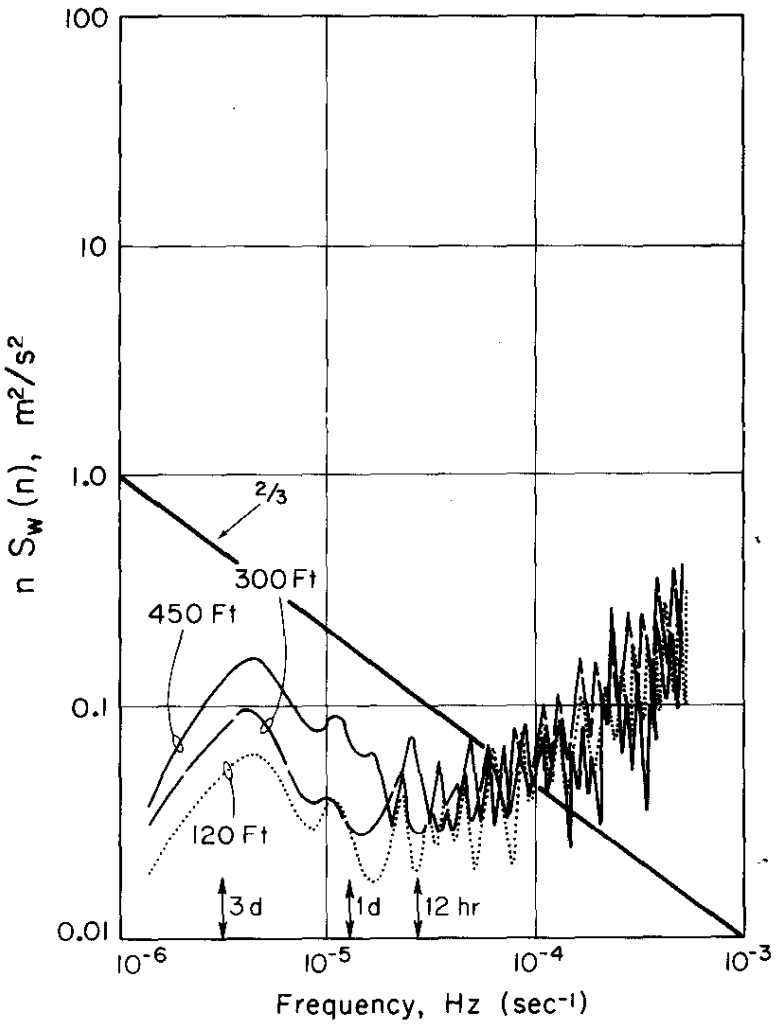

Figure 4-9. Kinetic Energy Spectra of Vertical Component, $\bar{w}$.

The third major peak is centered near a period of 12 hours. These semi-diurnal peaks are most prominent on the v-spectra and least noticeable on the speed spectra. The probable cause for this peak is wind direction fluctuations, primarily affecting the v-component. The only peaks at this frequency for the u-spectra are at the 800-ft level.

CONCLUSIONS

The effect of a mesoscale gap (having characteristics similar to those observed at the Savannah River Plant) on the diffusion of a typical puff release is shown to be significant for travel times greater than 1 hour. During periods exhibiting a gap, concentrations could be several decades higher than would be the case for periods having no mesoscale gap.

Analyses of mean kinetic energy spectra for 15 different time series show that similarity theory predictions may be applicable at a height of 300 ft at SRP. The decrease of kinetic energy with increasing frequency falls off at a rate faster than similarity theory predicts at levels above 300 ft and falls off at a rate slower than similarity theory predicts at levels below 300 ft. A reasonable explanation for this is that mechanical and convective turbulence at high frequencies decreases with increasing elevation.

An analysis of kinetic energy spectra for a 30-day period containing frequent frontal passages has shown that:

a. Greatest energy is associated with synoptic scale motions at a period of 3 days. For most levels, more energy is associated with the vector components than with the scalar wind speed indicating most of the velocity fluctuations associated with synoptic changes are in the wind direction.

b. The second largest spectral peak is associated with the diurnal cycle having a period of one day. Diurnal peaks in the spectra for the u and v components are about the same magnitude as the scalar speed spectra indicating the importance of wind speed in the diurnal peak.

c. A third peak is centered near a period of 12 hours. This peak is most prominent on the v spectra and least noticeable on the scalar wind speed spectra. This peak is apparently caused by direction fluctuations.

d. The kinetic energy spectra for the three components of the wind vector suggest that the winds are nearly isotropic during periods of 1/2 hour.

REFERENCES

1. J. Van der Hoven. "Power of Horizontal Wind Speed in the Frequency Range from 0.0007 to 900 cycles per hour." *J. Meteor. 14,* 160-164, (1957).

2. N. K. Vinnichenko. "The Kinetic Energy Spectrum in the Free Atmosphere - 1 sec to 5 years." *Tellus. 22,* 158-166 (1970).

3. A. N. Kolmogoroff. "The Local Structure of Turbulence in Incompressible Viscous Fluids for Very Large Reynolds Numbers." *C. R. Acad. U.R.S.S. 30,* 301-305 (1941).

4. T. V. Crawford. *A Computer Program for Calculating the Atmospheric Dispersion of Large Clouds.* USAEC Report UCRL-50179, Lawrence Radiation Laboratory, Livermore, California (1966).

5. R. B. Blackman and J. W. Tukey. *The Measurement of Power Spectra.* Dover Publications, New York (1958).

6. F. Fieldler and H. A. Panofsky. "Atmospheric Scales and Spectral Gaps." *Bul. Amer. Meteorol. Soc. 51,* 1,114-1,119 (1970).

7. L. Wendell. "Some Diagnostic Applications of Wind Speed and Component Spectra for Mesoscale through Synoptic Scale Frequencies," *Proceedings of the Symposium on Air Pollution Turbulence and Diffusion, December 7-10, 1971.* H. W. Church and R. E. Luna, Editors. USAEC Conference Report SC-M-710913, Sandia Laboratories, Sandia, New Mexico.

5. EDDY DIFFUSIVITY AS A FUNCTION OF HEIGHT FROM TV TOWER TEMPERATURE DATA†

INTRODUCTION

Until recently, most attention has been given to atmospheric transport and diffusion over distances less than 10 km. Many approaches have been followed to predict concentrations as a function of distance from the source. All methods require a means by which the rate of dispersion can be approximated, such as a) eddy diffusivities,or b) coefficients relating plume dimensions to downwind distance and meteorological conditions. The former have been supplied through research and measurements in the lowest 50 m of the atmosphere with instrumented towers, and the latter have been supplied with crosswind arcs of samples located downwind from a source of a continuous plume of known emission rate. Proceeding to longer distance scales or to situations different from the plume studies requires knowledge of the eddy diffusivity through the greater depths of the planetary boundary layer. This is true whether one solves the various forms of the diffusion equation, or whether one uses particle-in-cell techniques to calculate regional air pollution. This latter technique avoids the numerical diffusion problems associated with numerical solutions of the diffusion equation and is exemplified in the work of Sklarew[1] and the current work of Lange[2] at Lawrence Livermore Laboratory. Lange[2] has developed a particle-in-cell computer model for calculating diffusion in shear flow.

On the larger scale, the work by Crawford[3] in modeling and verifying concentrations in large nuclear debris clouds for up to several days downwind also involved the input of an eddy diffusivity as a function of height in the boundary layer. The basis for the eddy diffusivity input data that Crawford used in his calculations was the analyses by Wong and Brundidge,[4] who estimated the eddy diffusivity as a function of height and time of day from the Texas tower data.

The purpose of this report is to perform an eddy diffusivity analysis for the first time for the Savannah River site, using temperature data collected between 1966-1968 at eleven heights on a 1200-foot instrumented TV tower located 15 miles from the plant site.

---

† Work done by T. V. Crawford and M. M. Pendergast

METHOD OF ANALYSIS

The two years of temperature data obtained as spot samples every three minutes was averaged into 15-minute units. Monthly averages of temperature were prepared for each 15-minute unit for each height. All weather conditions were included rather than the conventional procedure of using clear sky data only. Examination of these data revealed that the absolute accuracy of the temperatures was not sufficient to justify taking second derivatives of the temperature with height. Wong and Brundidge[4] had used these second derivatives and the change of temperature with time to calculate the vertical eddy diffusivity (K_Z) under the assumption of no atmospheric radiation effects on the temperatures. Therefore, estimates for K_Z at SRP were prepared using the time-lag-with-height for the occurrence of the temperature minimum, the time-lag-with-height for the occurrence of temperature maximum, and the decay-with-height of the amplitude of the diurnal temperature wave. The methods of analysis are outlined by Sutton,[5] and are not sensitive to the absolute accuracy of individual temperature sensors.

If the surface temperature can be described by a periodic wave, and if K_Z within a layer can be assumed constant, then the conduction equation can be used to evaluate K_Z from the diurnal temperature wave. More specifically, K_Z can be determined by evaluating $\partial t_{min}/\partial z$, $\partial t_{max}/\partial z$, and $\partial A/\partial z$ in each layer, where t_{min} is the time of occurrence of minimum temperature, t_{max} is the time of occurrence of maximum temperature, and A is the amplitude of the temperature wave.

A, t_{min}, and t_{max} were determined for each month (at each level) and then combined into seasonal averages with each season representing the average of six separate monthly values. This provided a modest amount of smoothing of the data, while still permitting the seasonal variation of K_Z to be examined. Additional smoothing of the data was accomplished by plotting t_{min}, t_{max}, and A as a function of the logarithm of height for each season. These plots are presented as Figures 5-1 through 5-4 for the spring, summer, fall, and winter seasons, respectively. A smooth line was drawn through the data points. Values taken from these lines were later used in the calculations of the K_Z's.

Figures 5-1 through 5-4 show that the largest amplitude of the diurnal temperature wave occurs in the fall season. Fall is consistently the season of least rain and yet it is still relatively warm. The smallest amplitude of the diurnal temperature wave is observed in the summer. Late afternoon cloudiness and thunderstorms tend to reduce the maximum temperatures, and

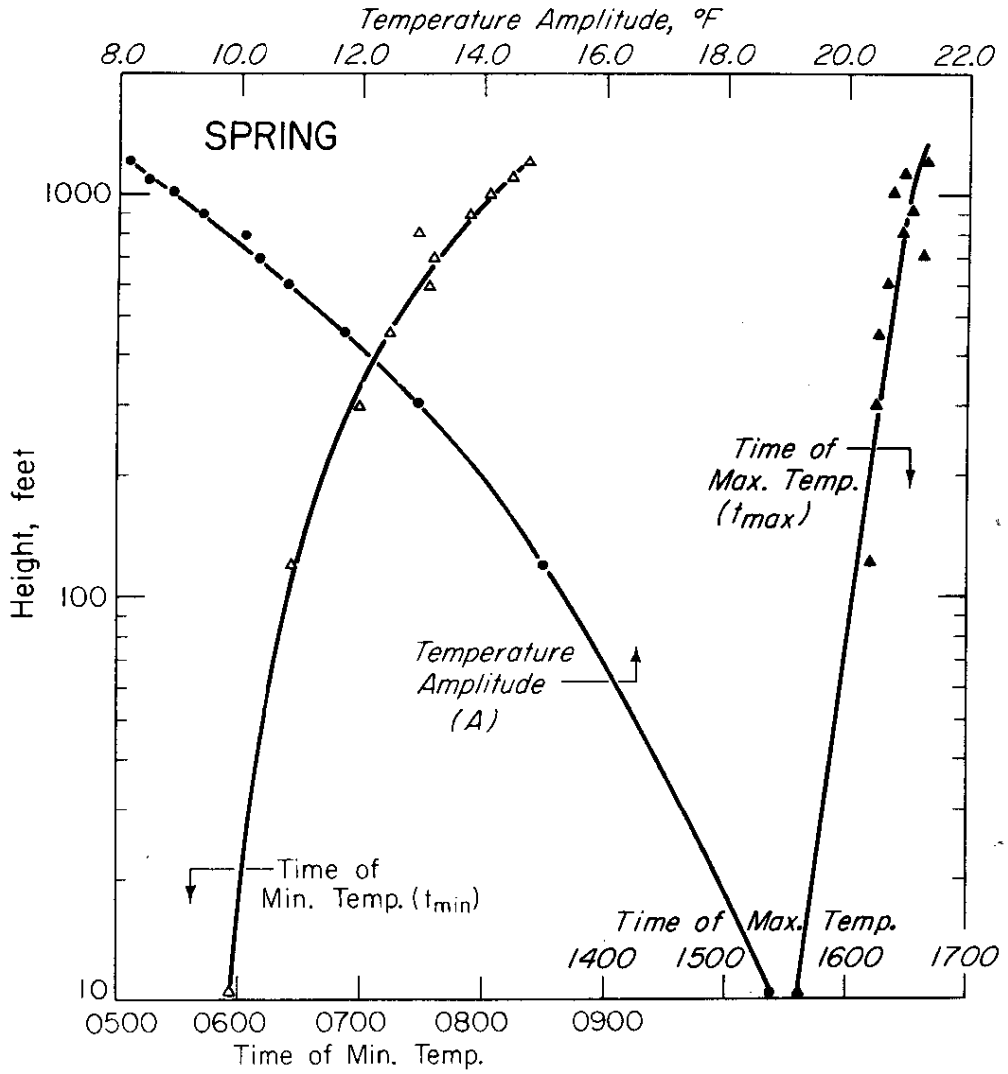

Figure 5-1. Time of Occurrence of the Minimum Temperature, Maximum Temperature, and the Temperature Wave Amplitude as a Function of Height for the Spring.

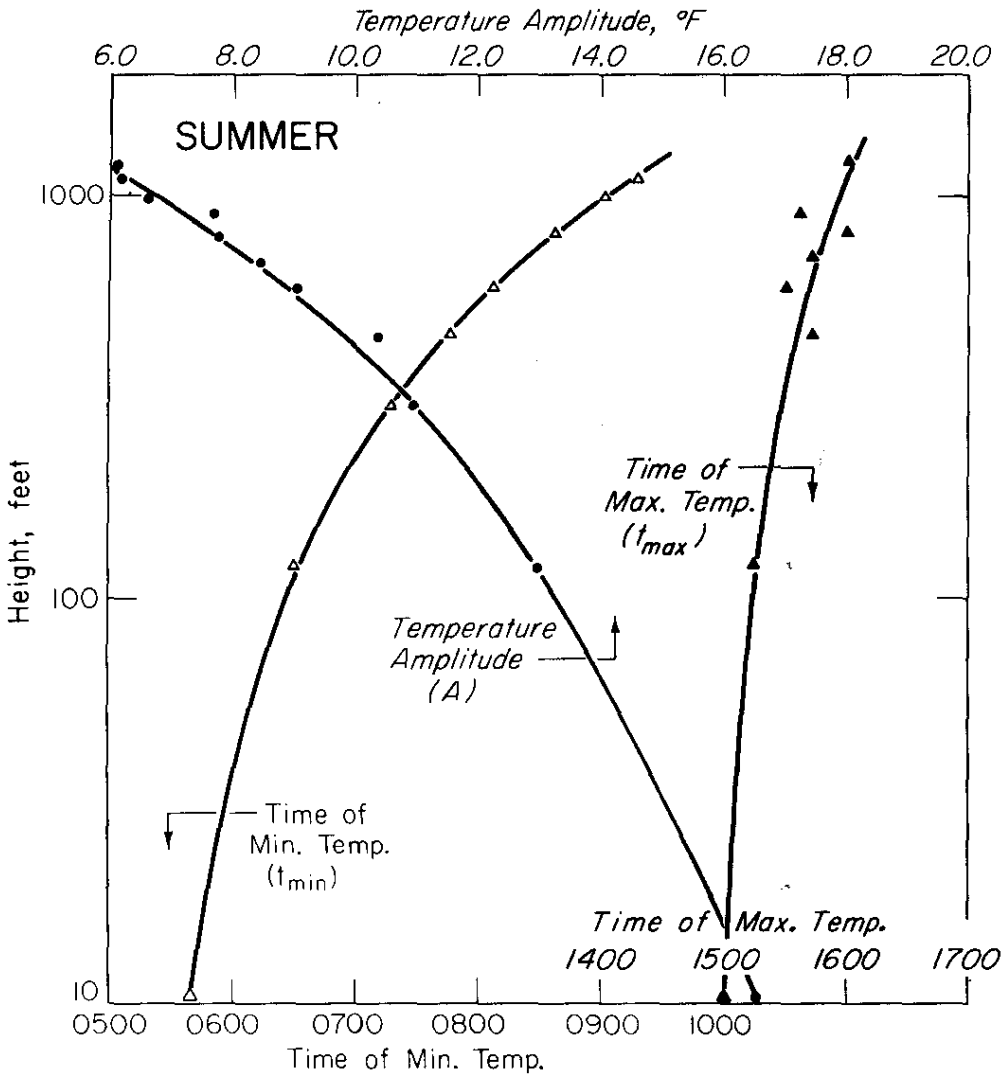

Figure 5-2. Time of Occurrence of the Minimum Temperature, Maximum Temperature, and the Temperature Wave Amplitude as a Function of Height for the Summer.

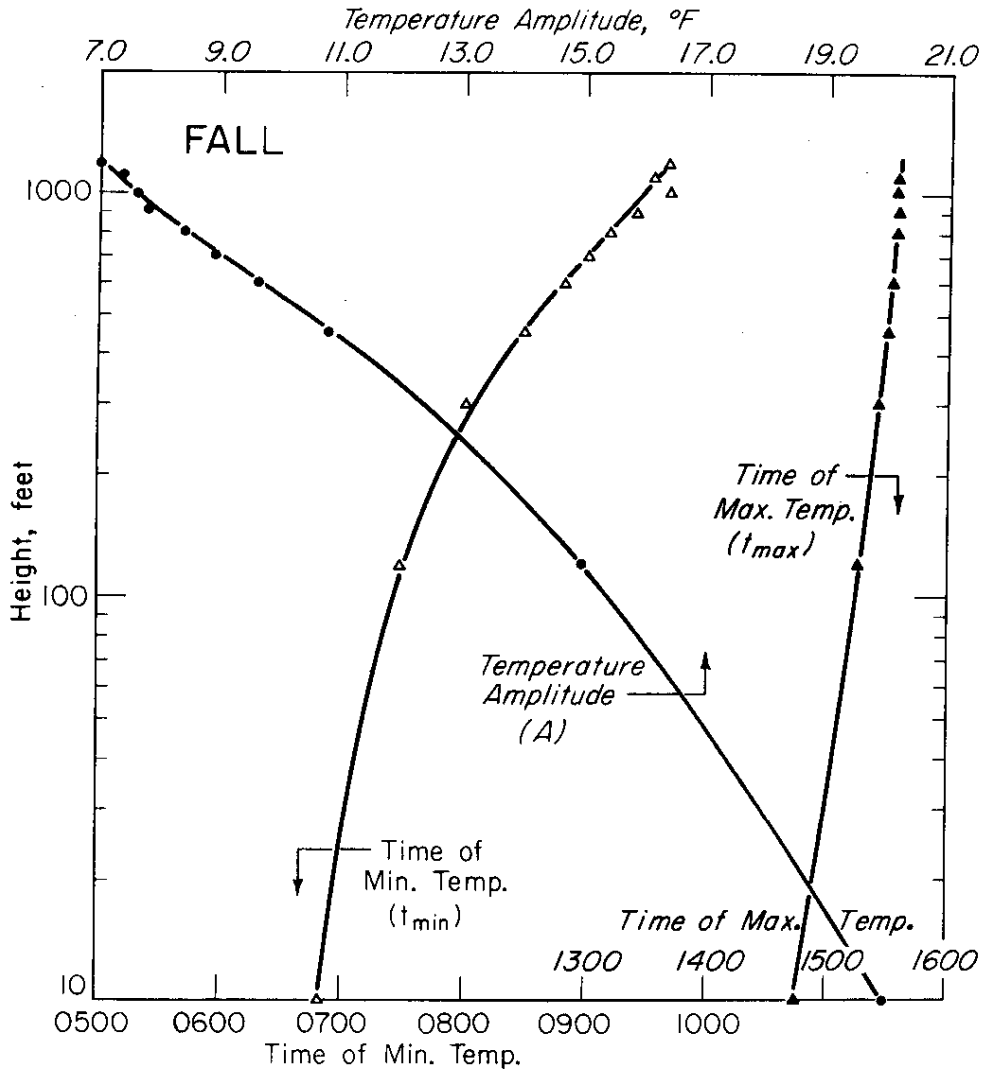

Figure 5-3. Time of Occurrence of the Minimum Temperature, Maximum Temperature, and the Temperature Wave Amplitude as a Function of Height for the Fall.

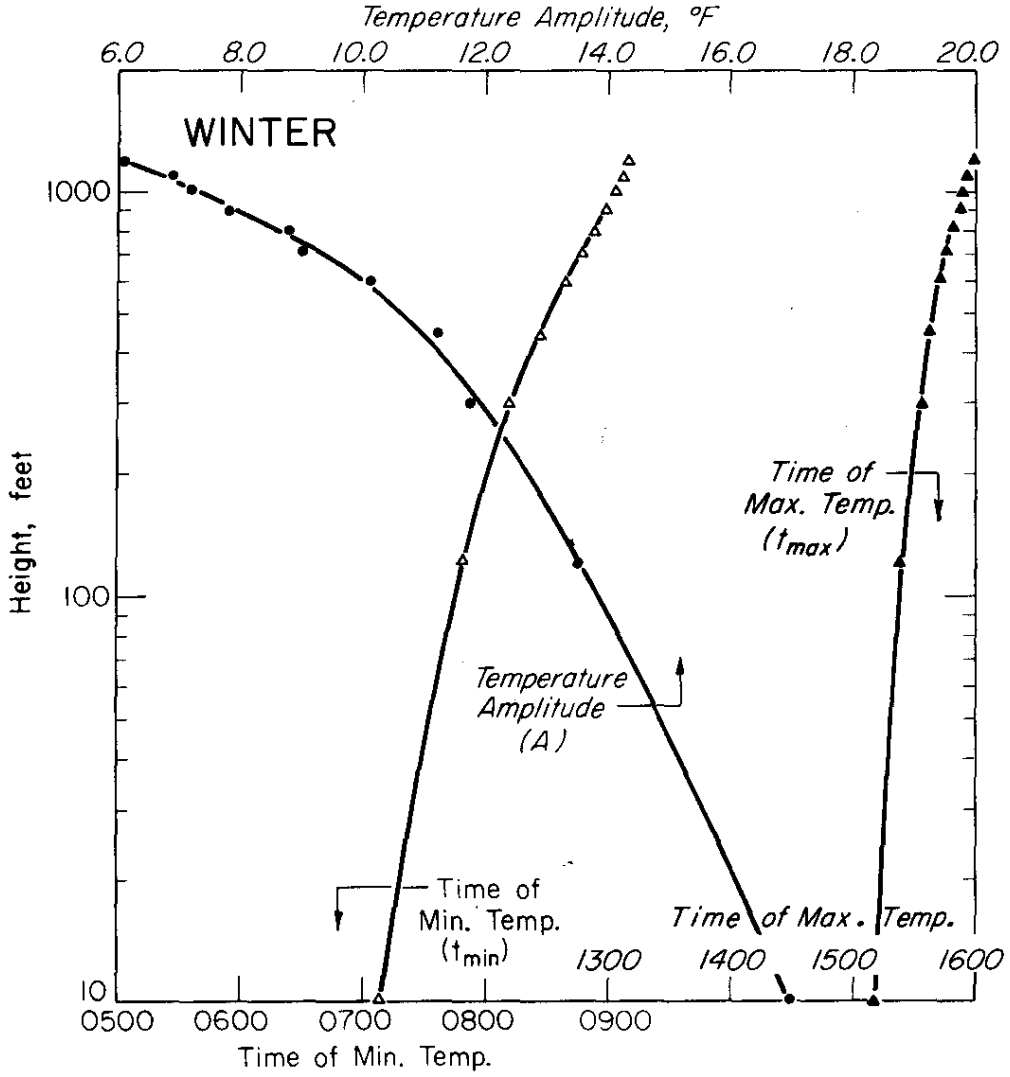

Figure 5-4. Time of Occurrence of the Minimum Temperature, Maximum Temperature, and the Temperature Wave Amplitude as a Function of Height for the Winter.

large amounts of water vapor in the lowest five thousand feet prevent much cooling at night. The shape of the temperature amplitude with height is similar for all seasons except for the fall when it decreases somewhat faster than during other seasons in the lower 300 feet. It decreases fastest during the winter season at heights above 700 feet.

The t_{min} is earliest in the summer and latest in the winter showing the expected correlation with the time of sunrise. There is a two (winter) to four (summer) hour time lag between the occurrence of the minimum temperature at the bottom of the tower and its occurrence at the top of the tower. This early morning time lag contrasts sharply with the late afternoon time lag for the maximum temperature, which is about an hour or less over the total height of the tower. This decreased time lag reflects the greater mixing of air in the afternoon than in the morning. The time of the maximum temperature occurs around three o'clock in the afternoon and occurs earliest in the fall and latest in the spring.

The K_z's calculated by using input from Figures 5-1 through 5-4 are shown in Table 5-I. The height values in the left hand column represent the actual heights at which input data from Figures 5-1 through 5-4 were taken for the calculations. Therefore, the eddy diffusivities represent averages over the indicated height ranges. Values are presented to one significant figure only as the data and methodology do not justify any greater precision.

The table reveals that the largest eddy diffusivities are determined from $\partial t_{max}/\partial z$. This relationship is physically consistent with the occurrence of maximum vertical mixing of air at the time of maximum temperatures in the afternoons. The eddy diffusivities obtained from $\partial t_{min}/\partial z$ are much smaller. These values are also closer to the eddy diffusivities obtained from $\partial A/\partial z$, representing an eddy diffusivity averaged over the 24-hour period. This similarity in values is physically consistent, as the atmosphere is stable a much larger fraction of the day than it is unstable.

Summarizing, examination of these data for seasonal trends shows:

- The use of $\partial A/\partial z$ indicates maximum eddy diffusivities occur in the spring and fall.
- The use of $\partial t_{min}/\partial z$ indicates maximum eddy diffusivities during the winter near the top of the tower and during the spring and fall at low heights.
- Use of $\partial t_{max}/\partial z$ indicates a high value of eddy diffusivity during the fall near the top of the tower and during the summer and winter at low heights.

Table 5-I. Eddy Diffusivities Calculated by Three Methods

Height, ft.	Calculated By Amplitude Decay ($\partial A/\partial z$), cm^2/sec	Calculated By Time Lag of Minimum Temperature ($\partial t_{min}/\partial z$), cm^2/sec	Calculated By Time Lag of Maximum Temperature ($\partial t_{max}/\partial z$), cm^2/sec
Spring			
10 - 30	2 (3)[a]	5 (3)	6 (3)
30 - 70	8 (3)	2 (4)	2 (4)
70 - 100	2 (4)	4 (4)	5 (4)
100 - 300	5 (4)	5 (4)	3 (5)
300 - 700	9 (4)	2 (5)	3 (6)
700 - 1000	1 (5)	2 (5)	7 (6)
1000 - 1200	2 (5)	2 (5)	3 (6)
Summer			
10 - 30	2 (3)	1 (3)	4 (4)
30 - 70	6 (3)	1 (4)	8 (4)
70 - 100	2 (4)	2 (4)	2 (5)
100 - 300	4 (4)	3 (4)	3 (5)
300 - 700	7 (4)	7 (4)	6 (5)
700 - 1000	8 (4)	1 (5)	2 (6)
1000 - 1200	7 (4)	1 (5)	4 (6)
Fall			
10 - 30	1 (3)	5 (3)	4 (3)
30 - 70	5 (3)	1 (4)	3 (4)
70 - 100	1 (4)	3 (4)	7 (4)
100 - 300	3 (4)	4 (4)	5 (5)
300 - 700	5 (4)	9 (4)	4 (6)
700 - 1000	1 (5)	2 (5)	5 (7)
1000 - 1200	2 (5)	3 (5)	5 (7)
Winter			
10 - 30	2 (3)	2 (3)	2 (4)
30 - 70	8 (3)	1 (4)	2 (5)
70 - 100	2 (4)	5 (4)	2 (5)
100 - 300	6 (4)	1 (5)	6 (5)
300 - 700	9 (4)	2 (5)	2 (6)
700 - 1000	5 (4)	7 (5)	3 (6)
1000 - 1200	4 (4)	9 (5)	2 (6)

a. $2\ (3) = 2 \times 10^3$

CONCLUSIONS

Seasonal temperature data from a 1200-foot TV tower near the Savannah River site were used to determine seasonal vertical eddy diffusivities using three different methods. The values for K_z are typical of those reported by others (for instance, by Wong and Brundidge[4]), i.e., about 10^3 to 10^4 cm^2/sec near the earth's surface, and about 10^4 to 10^6 cm^2/sec at 1000 feet above the ground. These data also show the expected diurnal variations; the values are larger during the afternoon than during the early morning. For time- and distance-dependent diffusion calculations, the above values will provide upper boundary limits for K_z for the Savannah River site.

REFERENCES

1. R. C. Sklarew, H. A. Fabrick, and J. E. Prager. *A Particle-In-Cell Method for Numerical Solution of the Atmospheric Diffusion Equation, and Applications to Air Pollution Problems.* Report 3SR-844, Volume 1, Final Report for the Division of Meteorology, National Environmental Research Center, Research Triangle Park, North Carolina, under EPA Contract No. 68-02-0006, (1971).

2. Personal Communication with Rolf Lange, Lawrence Livermore Laboratory, July 1973.

3. T. V. Crawford, *A Computer Program for Calculating the Atmospheric Dispersion of Large Clouds.* USAEC Report No. UCRL 50179, Lawrence Livermore Laboratory, Livermore, California (1966).

4. E. Y. J. Wong and K. C. Brundidge. "Vertical and Temporal Distributions of the Heat Conductivity and Flux." *J. of Atmos. Sci. 23,* 167-178 (1966).

5. O. G. Sutton. *Micrometeorology.* McGraw-Hill, New York (1953).

6. CURVED TRAJECTORIES AND DISPERSION CLIMATOLOGY USING WIND DATA OBTAINED AT A SINGLE TOWER†

INTRODUCTION

As described elsewhere in this report (Sections 2 and 7), the calculational procedures presently utilized at SRP include several assumptions concerning the meterological input. One assumption is that the wind velocity remains constant for the averaging time of the calculations. This commonly used assumption is reasonable for short periods of time (<1 hour), but not for longer travel times. For example, χ/Q values[a] at a distance of 100 km were obtained by assuming that the wind velocity existing when the parcel was released is identical to that affecting the parcel approximately 6 hours later. Naturally, if the wind velocity[b] changes during the 6-hour period, either temporarily or spatially, the parcel would not follow a straight trajectory but would follow a curved trajectory.

Because the presently utilized annual average χ/Q assumes uniform distribution over a 22-1/2 degree sector, small changes in wind direction would not appreciably alter the resulting χ/Q distributions. Large changes in direction could be significant, however, in that the parcel's χ/Q would be averaged over a different sector than that indicated by the straight trajectory. The network of instrumented towers to be established at SRP will be used to evaluate the differences between χ/Q patterns using the Gaussian plume model and curved and straight trajectories. In the meantime, differences will be investigated between time-dependent (but spatially constant) trajectories, and those with neither time nor space dependence.

Johnston and Lowry[1] outlined a procedure to compute a climatology of dispersion from sequential wind observations made at a single station. The technique is quite simple and assumes that

---

† Work done by M. M. Pendergast.

a. X/Q is defined as relative concentration, i.e., the ratio fo the ground level concentration (X) to the total emission (Q) of an airborne substance.

b. A change in wind velocity can arise from changes in wind speed or wind direction.

the wind measured at a single point is representative of the winds in the surrounding area, i.e., no spatial variation of wind. This technique results in curved trajectories and was applied to existing WJBF-TV tower data near SRP for comparison with existing calculations based on straight line trajectories. The calculation code is described, and dispersion climates obtained from several elevations at the WJBF TV tower are discussed.

CALCULATION METHOD

Wind trajectories of various durations were computed by vector addition of the average hourly wind vectors. An example of the calculation scheme for 3 hypothetical puffs emitted from a source located at point 0 is shown in Figure 6-1. At the end of the first hour, puff no. 1 has moved from point 0 to point 1. At the end of hour 2, puff no. 1 has moved to point 2, and puff no. 2 has moved from the origin to point 2'. At the end of the third hour, the first puff has moved to point 3, the second puff has moved to point 3', and the third puff has moved to point 3". For a 24-hour period, 300 vector end points would be provided with 24 trajectories having travel times ranging from 1 to 24 hours.

A grid network was established consisting of areas defined by 36 radials at 10 degree intervals, and of circles with radii at 10 km increments. The computer code retained the positions of the end points, and accumulated the number of end points falling into each of the 36 sectors of the grid (Figure 6-2). For each radial direction, the number of end points at 10 km intervals was tabulated and expressed as a percentage of the total number of end points that fell in that particular sector.

Isopleths connecting equal percentage values along each radial were constructed to analyze the resulting distribution of end points. These end points represent points in space over which the puff passed during the 24-hour period. Thus, the isopleths labeled 80% define an area which contains 80% of the end points and, by analogy, which contains 80% of the effluent emitted at the origin and traveling as defined by the wind field indicated at the origin.

Two isopleth patterns associated with different wind regimes are shown in Figure 6-3. The outer circle entered on the figure has a radius equal to the total "run-of-the-wind" (the summation of the wind speeds over the 24-hour period). This circle represents maximum distance that a parcel could travel within the 24-hour period if wind direction was constant over the whole period. Figure 6-3a shows the results of a prevailing wind from the

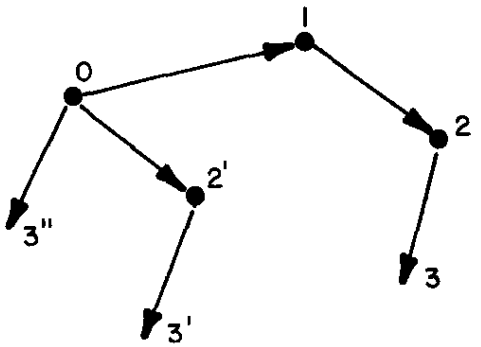

Figure 6-1. An Example of the Calculation Scheme for Three Hypothetical Puffs Emitted from a Source at Point 0.

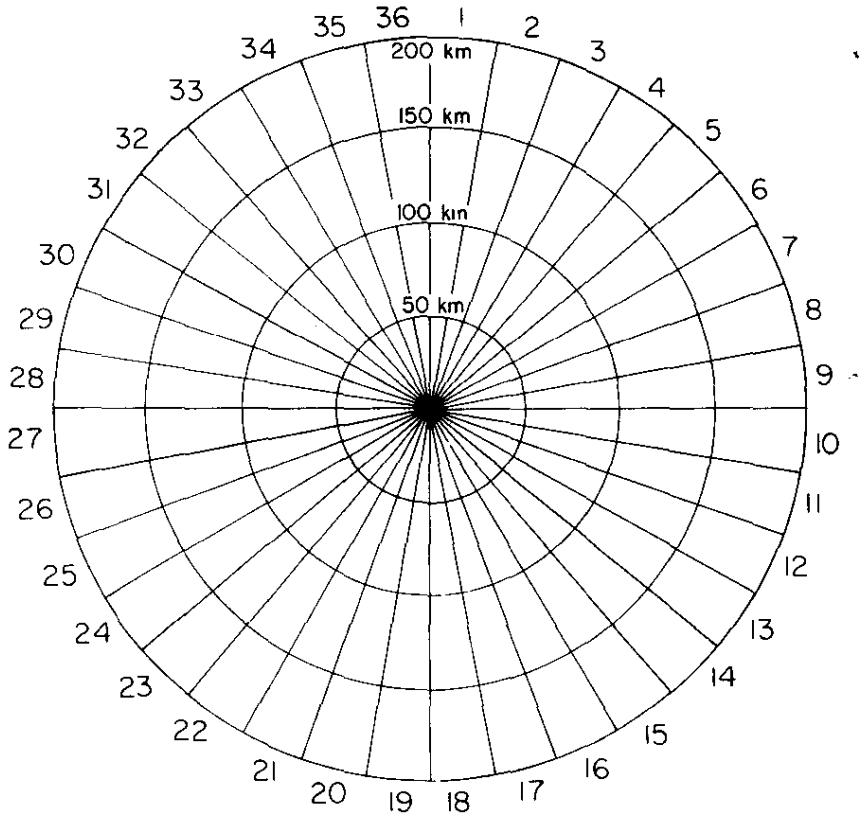

Figure 6-2. Grid Network to Accumulate the Position of End Points.

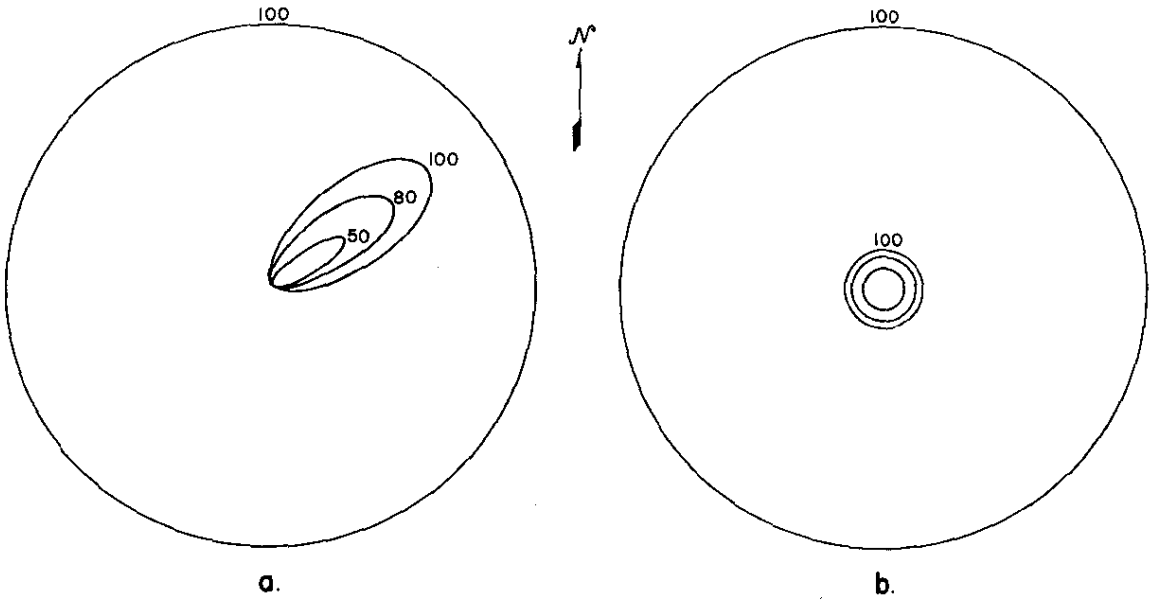

Figure 6-3. Isopleth Patterns Associated with Wind Conditions Leading to Two Different Dispersion Conditions.

southwest direction. The resulting isopleth pattern is oriented in a northeasterly direction, and, due to slight variation of wind direction, the 100% isopleth extends to about 80% of the maximum possible distance. Figure 6-3b shows a situation in which the total run-of-the-wind is identical, but continual change of wind direction has caused the end points to be clustered about the origin rather than extending in one direction.

The ratio of the areas of the corresponding isopleths for the two cases can be interpreted to indicate the relative magnitude of the dispersion characteristics of each wind regime. In this case, conditions leading to the isopleth pattern shown in Figure 6-3b would produce higher daily average concentrations than those shown in Figure 6-3a.

TRAJECTORY DISPERSION ESTIMATES FOR SRP

Dispersion estimates were obtained using the WJBF-TV tower data for one year beginning March 7, 1966. Trajectories of 6-hour duration beginning at 0000, 0600, 1200, and 1800 EST were computed using wind data averaged over 15-minute periods. A comparison of the area enclosed by the 100% isopleths for the four initial times and the six levels on the TV-tower can be used to obtain a relative dispersion climatology for SRP based upon wind direction and speed data only. Table 6-I gives the area

(in mi^2) enclosed by the 100% isopleth for 6-hour time periods at various tower elevations. These data indicate maximum dispersion of air parcels at 800 ft and minimum dispersion at 120 ft for all time periods. At the 120-ft level, the maximum dispersion occurs for the 6-hour period starting at 1800 EST, and minimum dispersion occurs at 0600 EST. At all other elevations, the maximum dispersion occurs for the 6-hour period starting at 0000 EST, and minimum dispersion occurs at 1200 EST. This observation reflects the existence of a nocturnal low-level jet stream.

The relative dispersion at the top of the tower is about four times greater than that at the bottom. The same distribution of stability categories and their associated plume dimension characteristics are assumed. The ratio of maximum dispersion divided by minimum dispersion at each level is entered in the last column of Table 6-I. The value increases from 1.5 at the 120-ft level to 6.1 at the 1000-ft level indicating the magnitude of the diurnal change in dispersion increases with increasing elevation.

Table 6-I. Dispersion Characteristics as a Function of Time of Day and Elevation Determined at the WJBF-TV Tower During the Period March 7, 1966, to March 7, 1967

Level, ft	Area Enclosed by 100% Isopleth at Various Elevations, mi^2				
	0000-0600	0600-1200	1200-1800	1800-2400	Max/Min
120	1,834	1,461	2,024	2,181	1.5
300	10,708	4,900	4,490	10,525	2.4
450	7,286	5,287	2,706	6,452	2.7
600	23,945	10,753	6,335	18,690	3.8
800	29,208	13,651	6,549	21,158	4.4
1000	22,608	9,353	3,689	16,444	6.1

CURVED VERSUS STRAIGHT TRAJECTORIES

An examination of six-hour trajectories was made using the same 15-minute average wind data shown in Table 6-I. Trajectories were calculated for the four 6-hour time periods at the 120 foot level (Figure 6-4). The solid lines delineate the maximum distance (the 100% isopleth) that a parcel would travel if emitted some time during each of the individual 6-hour periods. Parcels emitted at the beginning of the 6-hour period are assumed to travel further than parcels emitted toward the end of the period; and the solid line can be interpreted to represent the envelope of 6-hour "curved trajectories."

For comparison purposes, 6-hour straight-line trajectories were tabulated for the same time periods. These trajectories were calculated using the hourly average wind velocity at the initial time and assuming that this wind persisted for the entire 6-hour period. The maximum 6-hour straight trajectory envelopes during the one-year period for each 10-degree sector and each initial time are represented with dashed lines in Figure 6-4.

For the stable pollutant, this example indicates that the value of χ/Q at a particular location for the curved trajectory is 61% of the value for the straight-line trajectory for both points. For ^{41}Ar, the relative concentration for the curved trajectory is 55% and 34% of that given by the straight-line trajectory for 20 and 100 km, respectively.

The envelopes of the curved trajectories (solid lines) appear to be similar for all initial times with maximum displacement occurring towards the east and toward the southwest, with least displacement towards the south.

The envelopes of the corresponding straight-line trajectories (dashed lines) show general agreement with respect to wind directions associated with maximum displacement. The distances travelled in the straight-line trajectories are in general about 30% larger than the distance travelled assuming curved trajectories. The greater the difference, D, between the two, the greater is expected to be the effect of curvature on χ/Q at a particular location.

Relationships between curved and straight trajectories for 300, 450, 600, 800, and 1000 ft elevations were examined in a similar manner. For all cases, travel distances computed using straight line trajectories were larger than those using curved trajectories. Although a variation in D as a function of initial time and elevation was indicated, the scatter of points was too great to draw any meaningful conclusions.

The effect of this 30% increase in travel distance (or travel time if wind speed remains constant) on χ/Q calculations would be to reduce the values at all downwind distances. The consequent reduction in airborne pollution concentrations is explained by expansion of the plume with increasing distance from the source. For a radioactive pollutant, this 30% increase in travel time also allows additional radioactive decay to occur prior to reaching a particular point downwind.

An estimate of the probable magnitude of this reduction in concentration has been made for the above two cases. Since ^{41}Ar is the most significant gamma emitter released to the atmosphere (from an off-site dose standpoint, even though its contribution

to off-site population dose is only about 8% of the total) its half-life of 1.83 hours has been used in this example.

For a continuous point source and stability conditions corresponding to Pasquill type "C",[2] the values of χ/Q at plume centerline can be approximated by

$$\chi/Q = C\ x^{-1.85}$$

where x is total travel distance in km, and C is a constant depending upon the mean wind speed.[3] Values of χ/Q corresponding to straight and curved trajectories are shown for both cases for distances of 20 and 100 km from the source (Table 6-II).

Table 6-II. Magnitudes[a] of the Probable Effect of a 30% Increase in Travel Time-Distance on Pollutant Concentrations

	Stable Pollutant χ/Q			^{41}Ar $\chi/Q \exp(-0.693t/1.83)$		
	Straight	Curved	Curved/straight	Straight	Curved	Curved/straight
20 km (t = 1 hr)	3.9(-3)	2.4(-3)	0.61	2.67(-3)	1.47(-3)	0.55
100 km (t = 5 hr)	2.0(-4)	1.2(-4)	0.61	3.00(-5)	1.02(-5)	0.34

a. 3.9(-3) = 3.9×10^{-3}

CONCLUSIONS

1. An analysis of trajectories with 15-minute average winds for a one-year period indicates that 6-hour curved trajectories are at least 30% shorter than straight-line trajectories. If speeds are constant, this implies ∿30% greater travel time to reach a specific point and ∿40% lower value of χ/Q.

2. There was little difference in the direction dependence of curved versus straight-line trajectories.

3. Relative dispersion based upon distribution of trajectory end-points implies that the dispersion at the top of the tower is apparently ten times larger than that at the bottom (provided the same stability category distribution exists at both levels).

4. A diurnal variation of dispersion exists. The magnitude of this diurnal variation appears to increase with increasing elevation.

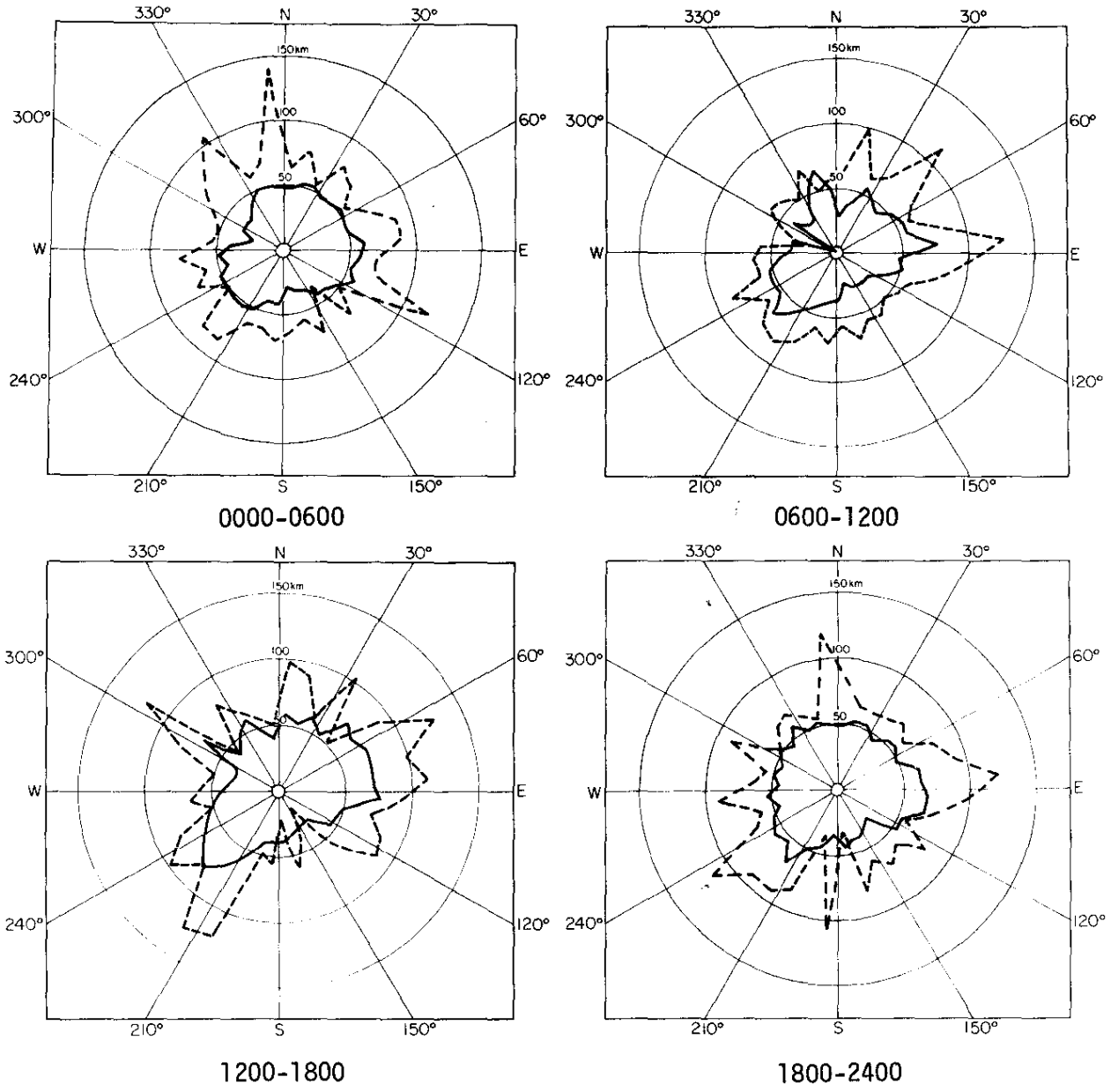

Figure 6-4. Envelopes of Curved (solid line) and Straight Line Trajectories (dashed line) for Four 6-hr Time Periods. Trajectories Were Calculated from Wind Data Obtained at the 120-ft Level of the WJBF-TV Tower for the Period March 7, 1966 through March 7, 1967.

5. The above example is illustrative of the effects for a particular day. It would not necessarily apply to population doses as concentrations at different distances along the trajectory (curved and straight) would have to be multiplied by appropriate populations, and the results integrated out to some distances from the site.

REFERENCES

1. R. E. Johnston and W. P. Lowry. "Computer Maps of Local Dispersion Climate Using Hourly Wind Sequences from a Single Station." Preprints, *Conference on Urban Environment* and *Second Conference on Biometeorology*, Philadelphia, Pennsylvania. Pp. 110-113, (1972).

2. F. Pasquill. "The Estimation of the Dispersion of Windborne Material." *Meteorol. Mag. 90* 1063 (1961).

3. D. H. Slade. *Meteorology and Atomic Energy 1968*. USAEC Division of Technical Information Report TID-24190, p 407 (1969).

7. A FRAMEWORK FOR CALCULATING DOSE-TO-MAN†

The Savannah River Plant (SRP) is a large nuclear complex engaged in varied activities. As a result of these activities, there are continuous and intermittent releases of radioactive gases to the atmosphere. Although SRP has an extensive monitoring system, an environmental model is needed to estimate potential effects of possible radioactive releases to the environment. The modeling system is required for basically two reasons: 1) the majority of releases are very low level and may not be detectable, and 2) accounting for all releases by monitoring methods alone is difficult, even if the releases were detectable. A model was developed based on measured and calculated releases, and dispersion by measured meteorology.

The environmental model in use at SRP is diagrammatically presented in Figure 7-1. The first objective in developing the model was to obtain a library of data representing annually averaged azimuthal and radial distributions of released material. This library was obtained for two separate paths: air concentrations at ground level for each isotope considered, and whole body dose estimates for discrete gamma energies that were spatially distributed.

The meteorological data were obtained from instrumentation installed on the WJBF-TV tower located approximately 30 km from the geometric center of SRP. For modeling purposes, the data origin was assumed to be translatable to any release point of interest within the general area, including offsite release points. The first phase of library construction left the data origin undefined. The second phase related calculated distributions to specific emission points.

Annually averaged air concentrations were estimated for each isotope individually by processing the meteorological data assuming a unit release (1 curie) for each data period (15 min or hourly averages). Ground level concentrations were accumulated as a function of azimuth and radial distance from an arbitrary origin and plotted on a grid overlay of the SRP and

---

† Work done by R. E. Cooper.

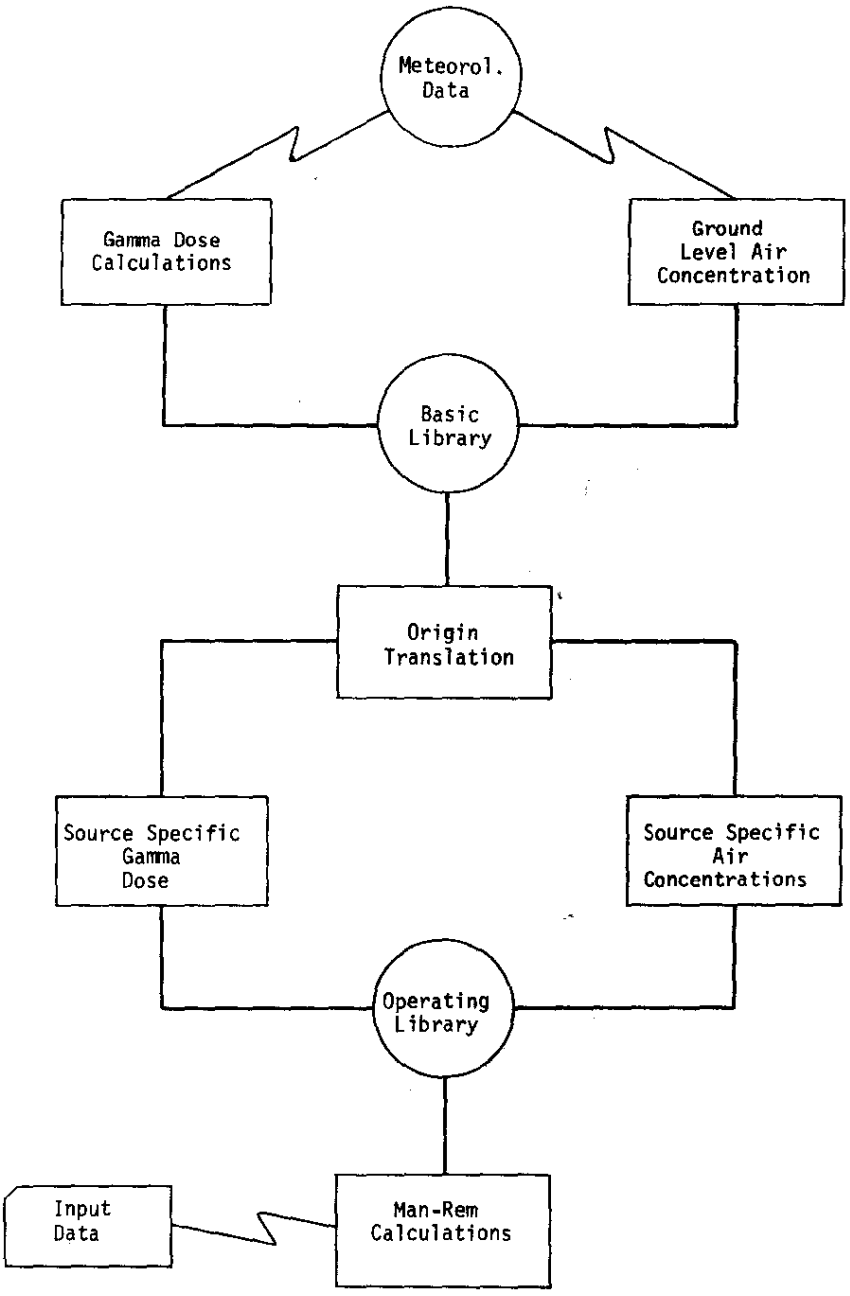

FIGURE 7-1. Man-Rem Calculation Procedures

environs. At the end of this procedure, i.e., after all meteorological data for the two-year period had been processed, the accumulated concentrations were divided by the total number of data periods represented. The result was a quantity representing a yearly integrated concentration associated with each grid point assuming a unit curie release over the year. These quantities were corrected for decay according to isotope and measured meteorology for each data period.

Whole body dose calculations were performed by processing the meteorological data in a similar fashion. However, the calculations were significantly more complex as the gamma dose to a receptor may be strongly dependent on the total spatial distribution about the receptor, and not necessarily related to ground level concentration. To minimize computations and at the same time have a library of data covering the usually encountered spectrum of gamma energies, the calculations were performed for discrete gamma energies instead of being isotope dependent. This also provided an efficient method of treating multiple energies from individual isotopes when desired.

Because the gamma calculations were isotope independent, the library data need not be corrected for decay, but a correction will be made when the data are utilized later as will be described. The gamma calculations are performed with the aid of EGAD,[1] a computer code developed at SRP for that purpose. The calculations are normalized to a unit curie release of discrete gamma energies over the range of 0.01 through 5.0 Mev.

After the above calculations are completed, the library consists of isotope and gamma energy data originating from an arbitrary point. To relate these data to a specific population grid to facilitate man-rem calculations, the library data are reprocessed. In this processing, each source to be treated as a separate entity is assumed to be the origin of material distributions, and a predetermined population grid is assumed to be exposed. Thus, a new library is constructed that contains annually averaged data that is source specific, but always with respect to the same fixed population grid.

Man-rem calculations are performed by processing the library data according to source point and release magnitude. Multiple source points may be considered within a single pass to estimate total man-rem exposure from sources separated by large (>100 km) distances. In addition, multiple gamma energies may be input for individual isotopic species. Decay corrections are then applied to the gamma calculations. Some of the isotopes being considered from each source point, particularly tritium and ^{85}Kr, may be assumed for practical purposes to have infinite half-lives over the time intervals of interest, i.e., transport times out

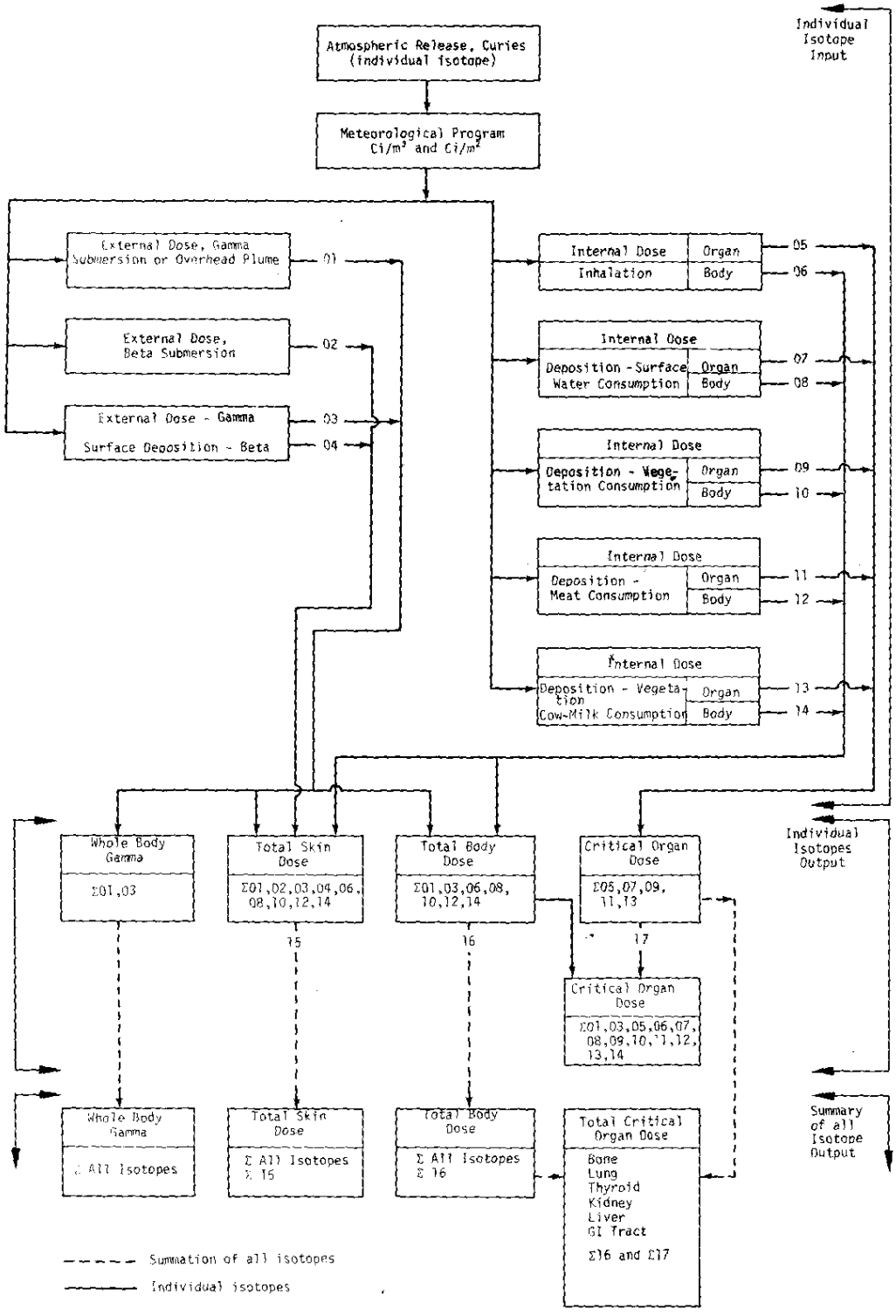

FIGURE 7-2. Atmospheric Release Model

to a maximum of 150 km. For any particular isotopic species whose decay is significant, a decay correction for each grid point is simply determined as the ratio of ground level concentrations with respect to a long-lived isotope from the same source.

The SRP program considers many atmospheric pathways to man (Figure 7-2). All pathways, except whole body gamma doses, have dose conversion factors relating all dose calculations to estimated ground level concentrations as contained in the library data.

REFERENCES

1. R. E. Cooper. *EGAD - A Computer Program to Compute Dose Integrals from External Gamma Emitters.* USAEC Report DP-1304, E. I. du Pont de Nemours and Co., Savannah River Laboratory, Aiken, S. C. (1972).

8. METEOROLOGY AND SULFUR DIOXIDE CONCENTRATIONS AT SRP†

INTRODUCTION

Although radioactive pollutants are a major concern at SRP, enough sulfur dioxide is emitted each year by the seven coal-fired power plants located onsite to warrant surveying for sulfur dioxide. The locations and annual emission rates for the seven sources are shown in Figure 8-1. The largest source is at D Area, and is also the sulfur dioxide source closest to the plant boundary. For this reason, D Area is the focal point for the sulfur dioxide survey.

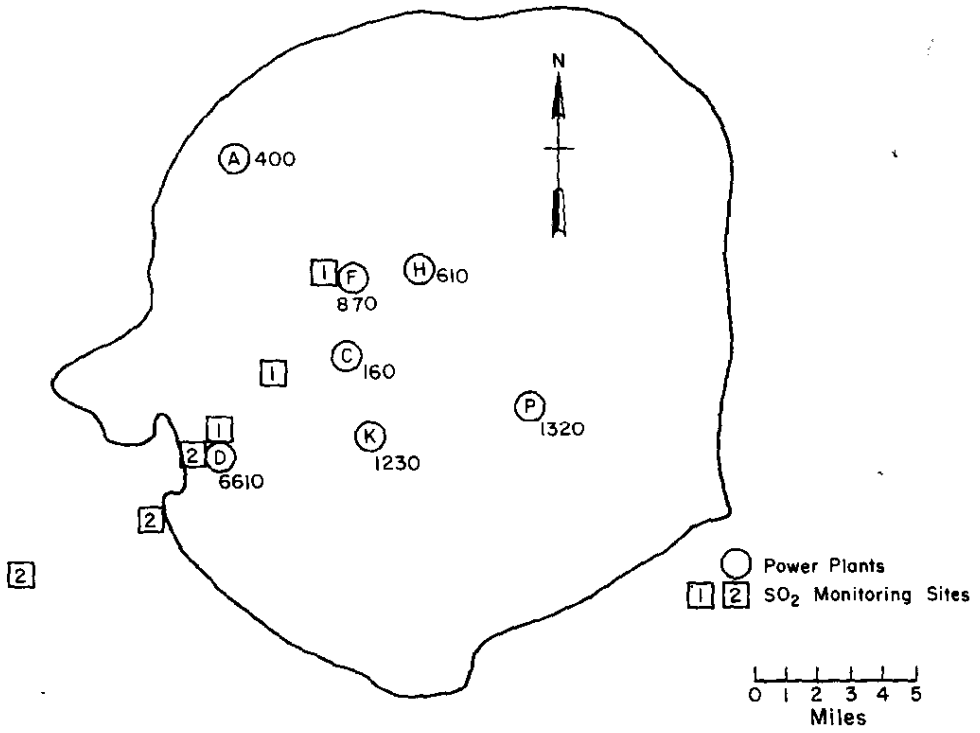

FIGURE 8-1. SRP Map. The seven coal-fired power plants at SRP and the average annual emissions of sulfur dioxide (in tons). Also shown are the sulfur dioxide monitoring sites for the onsite and offsite survey.

† Work done by M. M. Pendergast and E. L. Wilhite

The survey for sulfur dioxide at SRP is being carried out by a cooperative effort of three different groups. Personnel of the Environmental Effects Division (EED) of the Savannah River Laboratory (SRL) have provided the necessary support for the sulfur dioxide monitoring, calibration of instruments, and reduction of the sulfur dioxide data. SRP personnel have provided source-strength information and the majority of the meteorological data. Environmental Transport Division (ETD) personnel have performed much of the data reduction and are performing the analyses.

Calculations of offsite concentration were made using 2 years of meteorological data (obtained at the 1200-ft WJBF-TV tower located at Beech Island, South Carolina) and annual average sulfur dioxide emissions. These calculations indicated that state and federal air-quality standards could be exceeded.

The calculations indicate standards associated with short averaging times (an hour or a day) are the ones likely to be exceeded, and yet the only other comparisons with data have been on an annual average basis. Peak emissions, half-hour averages, and hourly averages are being tabulated in the current sulfur dioxide program. These sulfur dioxide measurements are being made to confirm (or disprove) that standards are not being exceeded; and to check with real data the calculational procedures used to determine the probability of exceeding these standards.

PLAN

This study is being accomplished in three phases: collection, calculation, and comparison. The collection phase consists of continuous measurements of sulfur dioxide at positions shown in Figure 8-1. The primary collection involves six months of continuous measurements between June and November 1973. A preliminary measurement program was carried out in April and May 1973.

The sulfur dioxide monitors will be located to the northeast of the D Area at distances of 1, 5, and 10 km for the first three months and then relocated to the southwest for the remainder of the survey. Climatologically, these two orientations offer the highest probability of passage of the D-Area plume over the monitoring sites. Incidentally, southwest winds in this area occur predominately during the daytime, and the speeds are stronger than for the northeast winds which prevail at night. Thus, the two monitoring configurations offer two different meteorological conditions to increase the probability of obtaining sulfur dioxide data representative of a wide spectrum of diffusion conditions.

The calculations and comparison phases of the study will not be fully implemented until all data are collected. Upon the completion of the data collection phase, calculations will be made using equations for a continuous point-source (with plume rise), and the results compared with observed values of sulfur-dioxide. These calculations will be made with WJBF-TV tower data only, and then with combined TV tower data and SRP operating area wind observations.

A discussion of the sulfur dioxide instrumentation and calibration procedures, and an analysis of the data collected during the preliminary study follows.

SULFUR DIOXIDE INSTRUMENTATION

At each site, an *Ultragas** U3S continuous sulfur dioxide analyzer is being used. The instruments operate on the conductimetric principle. The air sample is absorbed in a stream of reagent (dilute, acidified peroxide), and the change in conductivity of the reagent is measured and displayed on a strip chart recorder.

Each instrument was calibrated in the laboratory using National Bureau of Standards (NBS) certified permeation tubes. The permeation tube was enclosed in a glass tube, then immersed in a water bath at 27.7 ± 0.1 C. Air was passed through a calibrated dry test meter at a rate of 2880 ± 10 ml/min and then over the permeation tube and into the instrument. The permeation rate of the tube at this temperature is 722 ± 4 ng SO_2/min. The expected concentration was, therefore, 0.095 ppm. Each of the three instruments agreed with the expected value to within 5%.

The calibrated instruments were located in the field and are serviced on Mondays and Fridays. The servicing involves changing charts, replenishing reagent, and performing routine maintenance. Strip charts are visually examined to obtain 0.5-hour average values and peak values. These data are punched onto cards for later statistical analyses.

PRELIMINARY STUDY

Data were collected and reduced during the checkout of the sulfur dioxide monitor. Hourly average values of sulfur dioxide concentrations at a distance of 1 km from the D-Area stacks and

* Product of H. Woesthoff, oHG., Bochum, Germany. Distributed by Calibrated Instruments, Inc., Ardsley, N. Y.

hourly average wind data were obtained during April and May. The analysis of these data has accomplished several objectives:

1. Testing of methods for the reduction of sulfur dioxide and wind data were accomplished.
2. Some knowledge of local winds in D Area were obtained.
3. An insight into the possible effects of other SRP sulfur dioxide sources was gained.

During the months of April and May 1973, strip chart records of wind velocity were available at two locations in the D Area. A portable wind instrument and stand, hereafter referred to as MRI, was positioned approximately 6 m from the sulfur dioxide analyzer at an elevation of 3 m above the ground. The second was located at the top of the 40 m "bubble tower" (Building 412-D) which will be referred to as BUB. The locations of the wind instruments are depicted in Figure 8-2. A wind direction of 218° would cause a plume emitted from the power plant stacks to pass directly over the sulfur dioxide monitor, provided the plume follows a straight line path.

A scatter diagram (Figure 8-3) shows the relationship between hourly average wind directions (rounded to the nearest 10 degrees) measured at BUB and MRI during the preliminary program. The diagonal line represents the loci of points when both directions are equal. The plotted numbers show the number of times each combination of wind directions occurred. On the average, the direction indicated at BUB is shifted approximately 20 degrees clockwise from the corresponding MRI direction. For approximately 40% of the time, however, differences between observed directions exceed 50 degrees. The major causes for the observed differences are:

1. Greatest differences occur when BUB wind speed is less than 5 mph, i.e., when wind directions are more variable.
2. When the wind is from the south to southeast, the MRI instrument is downwind of the columns (Buildings 410-D through 414-D), and the induced wake causes large differences in wind directions.
3. During stable conditions, which normally occur at night, significant decoupling in the vertical occurs, causing surface wind velocities to be significantly different from wind velocities located at 40 m above the surface.

A frequency distribution of 1-hour average sulfur dioxide concentrations at Bldg. 614-D (located within the D Area approximately 1 km to the northeast) during the period April 1 through May 14 was plotted on log-probability paper (Figure 8-4). The data follow a straight line which, by definition, means that

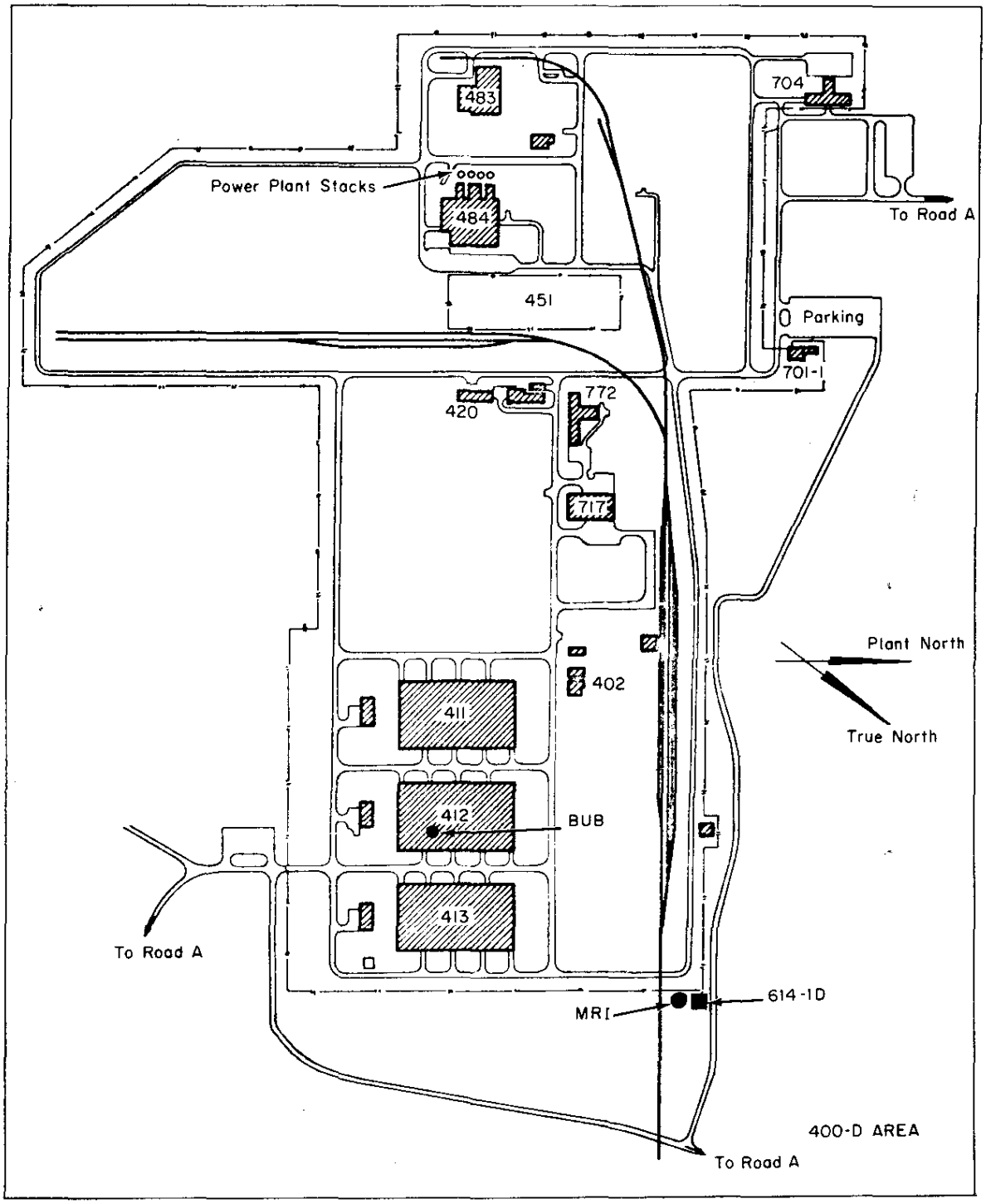

Figure 8-2. Map of D-Area Showing the Power Plant, Stacks, MRI, BUB, and Building 614-1D.

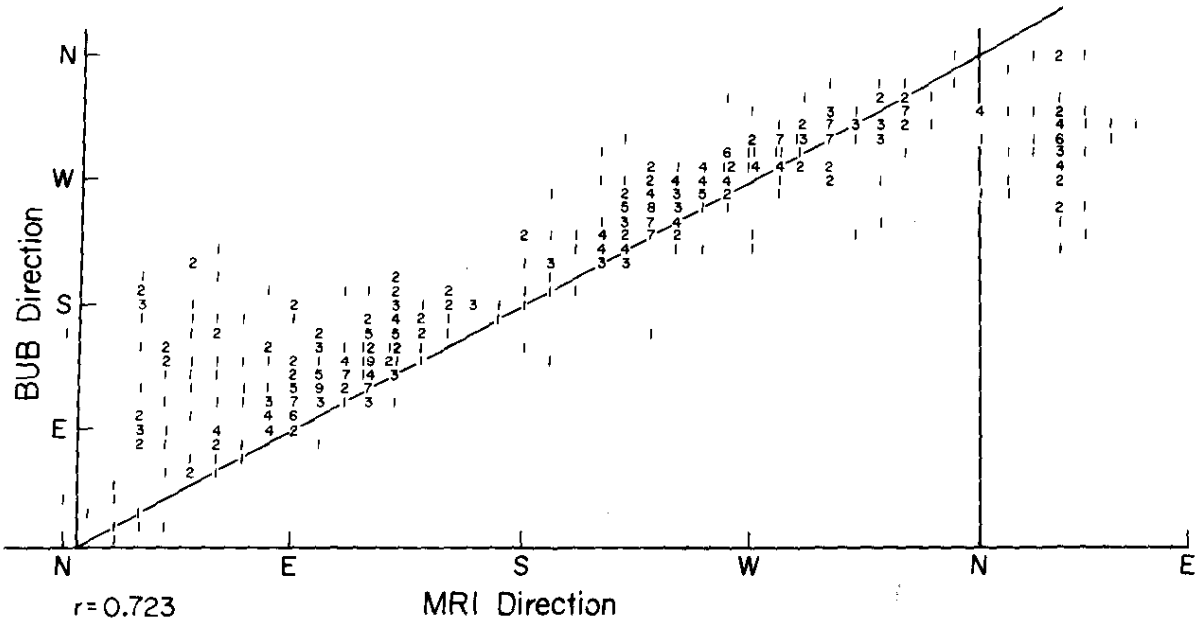

Figure 8-3. Scatter Diagram Showing Relationship Between Wind Directions from MRI and BUB. The Numbers Represent the Number of Occurrences of the Particular Wind Direction Combinations.

the sulfur dioxide data are lognormally distributed. Larsen[1] has established that air pollution concentration distributions measured at a point influenced by multiple sources follow the lognormal function. Thus, Figure 8-4 suggests that more than 40 percent of the time the sulfur dioxide concentrations measured at Bldg. 614-1D are from several sources because winds from the D-Area powerhouse to the sulfur dioxide measuring instrument occur with less than a 40 percent frequency (see Figure 8-3).

To test the above hypothesis, the relationship between wind direction and sulfur dioxide concentration was examined. The correlation between sulfur dioxide concentration with wind speed and direction at BUB is shown on Figure 8-5. The abscissa is wind direction to the nearest ten degrees, and the ordinate is wind speed in mph. Plotted on the graph is the average of the hourly average sulfur dioxide concentrations corresponding to each combination of wind speed and direction. Isopleths of 20, 40, and 60 ppb are sketched on the graph.

The concentration isopleth pattern depicts two major "plumes." The largest is associated with winds from the southwest with speeds in excess of 7 mph. For these conditions, the height of rise of the plume from D-Area power plant stacks is inhibited by the high wind speeds and is mixed to the ground as the result of mechanical turbulence.

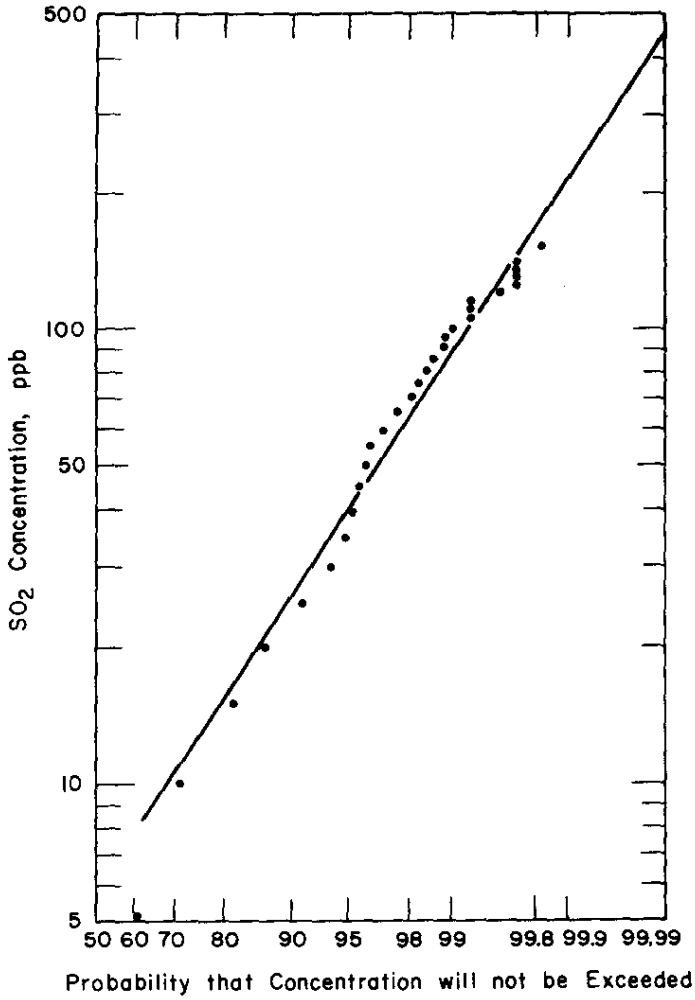

Figure 8-4. Frequency Distribution of 1-hr Average Sulfur Dioxide Concentrations at Building 604-1D During the Period April 1, through May 14, 1973.

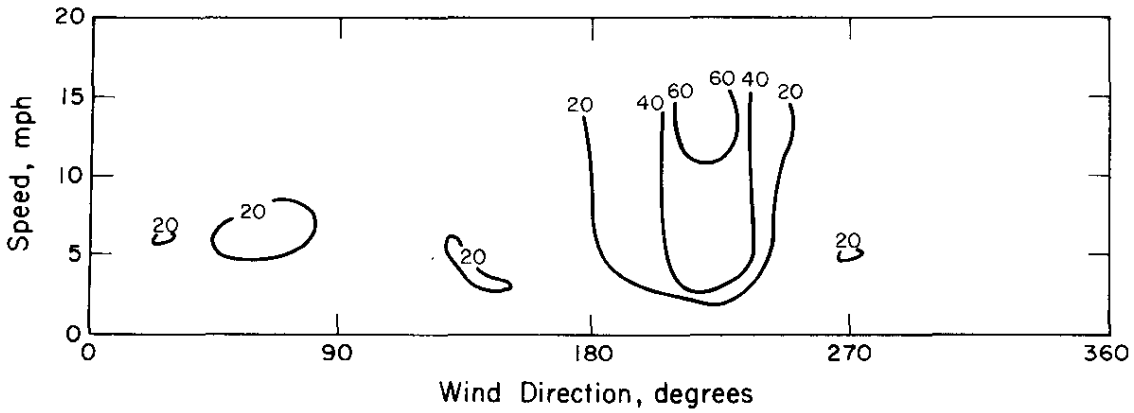

Figure 8-5. One-hour average sulfur dioxide concentrations (in ppb) measured at Bldg. 614-1D plotted versus wind speed and direction as measured at BUB.

The second plume corresponds to northeasterly winds and is probably from other sulfur dioxide sources, particularly in C and F Areas (see Figure 8-1). For this case, low wind speeds tend to produce the highest concentrations, because, for the travel distances involved (6-10 km), the plume has expanded sufficiently to be measured near the ground.

Wind statistics are presented for BUB and for the 110-ft level of Cassels Fire Tower located 5 km to the NE (Table 8-I). The Cassels data represent the average of the two periods April 7 through May 7, 1966,and April 7 through May 7, 1967.

Table 8-I. A Comparison of Wind Statistics between BUB and Cassels Fire Tower.

Wind Direction:	NNE	ENE	ESE	SSE	SSW	WSW	WNW	NNW
Cassels								
%	6.6	10.2	14.5	18.5	19.3	14.8	8.7	6.8
Speed, mph	4.6	4.5	4.2	4.4	4.7	5.5	5.7	4.2
BUB								
%	1.6	5.6	17.4	16.9	9.5	14.0	28.7	6.0
Speed, mph	4.9	4.9	6.2	7.2	5.3	7.5	7.5	5.5

The BUB wind data show a prevailing WNW wind with a secondary maximum from the southeast. The Cassels data indicate a prevailing southerly wind direction with SSE and SSW occurring with the highest frequency. Thus, the preliminary program survey may not be representative of "normal" wind conditions at D Area since the frequency of SSW and NNE winds was much less in April and May 1973 than indicated for the same months in 1966 and 1967.

CONCLUSIONS FROM PRELIMINARY PROGRAM

Although the prime purposes for this early effort were instrumentation and procedure checkout, some tentative conclusions have emerged. These are:

1. The sulfur dioxide concentrations are lognormally distributed in the D Area for those values above background.
2. High concentrations of sulfur dioxide at 1 km northeast from the D Area powerhouse are associated with :
   a. Strong southwest winds which force the D-Area powerhouse plume to the ground surface.
   b. Weak northeast winds which minimize the dilution rates of the sulfur dioxide plumes from the C- and F-Area powerhouses.
3. At 1 km to the northeast of the D-Area powerhouse, the sulfur dioxide concentrations associated with winds from the F and C Areas are about one third those associated with winds from the D Area.
4. Considerably more northwest and considerably less northeast and southwest winds were observed in April through May 1973 than during the same periods in 1966 and 1967.

REFERENCE

1. R. I. Larsen. "Relating Air Pollution Effects to Concentration and Control." *J. Air Pollution Control Assn. 20,* 214-225 (1970).

PRESENTATIONS

T. V. Crawford - A Seminar at North Carolina State University, Raleigh, North Carolina, on December 8, 1972.

T. V. Crawford - A Talk to the South Carolina Chapter of The American Nuclear Society in Aiken, South Carolina, on March 15, 1973.

T. V. Crawford - A Lecture as part of a "Short Course on Atmospheric Turbulence and Diffusion and Its Effect on Pollution" at the University of Tennessee Space Institute, Tullahoma, Tennessee, on April 5, 1973.

T. V. Crawford - A Talk to the South Carolina Chapter of The American Meteorological Society in Aiken, South Carolina, on May 17, 1973.

MEETINGS

T. V. Crawford	- American Meteorological Society *Workshop on Micro-Meteorology*, Boston, Massachusetts, August 14-18, 1972.
T. V. Crawford	- Division of Biomedical and Environmental Research, USAEC, Atmospheric Science Group Leaders Meeting, Gaithersberg, Maryland, September 27-28, 1972.
B. C. Rusche and T. V. Crawford	- *Inter-Agency Conference on the Environment* at the Lawrence Livermore Laboratory, Livermore, California, October 17-19, 1972.
R. E. Cooper, T. V. Crawford, and M. M. Pendergast	- *Symposium on the Statistical Aspects of Air Quality Data*, Chapel Hill, North Carolina, November 9-10, 1972
T. V. Crawford and M. M. Pendergast	- Visit to the Meteorology Groups at Argonne National Laboratory, Argonne, Illinois, and the Atmospheric Turbulence and Diffusion Laboratory, Oak Ridge, Tennessee, November 27-30, 1972.
T. V. Crawford	- *Third Chemist-Meteorologist Workshop* at Fort Lauderdale, Florida, January 15-19, 1973.
T. V. Crawford and B. C. Rusche	- Attended briefing by Lawrence Livermore Laboratory before the Directorate of Regulation, USAEC, Bethesda, Maryland, January 30, 1973.
T. V. Crawford	- Department of Transportation *Climatic Impact Assessment Program Working Meeting* at the National Center for Atmospheric Research, Boulder, Colorado, February 21-23, 1973.
J. C. Corey and T. V. Crawford	- Annual Information Meeting of the Environmental Sciences Division, Oak Ridge National Laboratory, Oak Ridge, Tennessee, March 26-27, 1973.

T. V. Crawford - Annual Information Meeting of the Atmospheric Sciences Group, Lawrence Livermore Laboratory, Livermore, California, May 2-3, 1973.

AES/sce